Report Prepared by:

Ezeddin R. Busba
Alberto A. Sagüés
Gray Mullins

FINAL REPORT

REINFORCED CONCRETE PIPE CRACKS – ACCEPTANCE CRITERIA

Contract No. BDK84 977-06
Final Report to Florida Department of Transportation

A. A. Sagüés
Principal Investigator
Department of Civil and Environmental Engineering

UNIVERSITY OF SOUTH FLORIDA
COLLEGE OF ENGINEERING

Tampa, FL 33620
July 1, 2011

(Revised July 29, 2011 – See p.73)

DISCLAIMER

The opinions, findings, and conclusions expressed in this publication are those of the authors and not necessarily those of the State of Florida Department of Transportation.

SI* (MODERN METRIC) CONVERSION FACTORS

APPROXIMATE CONVERSIONS TO SI UNITS

Symbol	When You Know	Multiply By	To Find	Symbol
		LENGTH		
in	inches	25.4	millimeters	mm
ft	feet	0.305	meters	m
yd	yards	0.914	meters	m
mi	miles	1.61	kilometers	km
		AREA		
in^2	square inches	645.2	square millimeters	mm^2
ft^2	square feet	0.093	square meters	m^2
yd^2	square yard	0.836	square meters	m^2
ac	acres	0.405	hectares	ha
mi^2	square miles	2.59	square kilometers	km^2
		VOLUME		
fl oz	fluid ounces	29.57	milliliters	mL
gal	gallons	3.785	liters	L
ft^3	cubic feet	0.028	cubic meters	m^3
yd^3	cubic yards	0.765	cubic meters	m^3
	NOTE: volumes greater than 1000 L shall be shown in m^3			
		MASS		
oz	ounces	28.35	grams	g
lb	pounds	0.454	kilograms	kg
T	short tons (2000 lb)	0.907	megagrams (or "metric ton")	Mg (or "t")
		TEMPERATURE (exact degrees)		
°F	Fahrenheit	5 (F-32)/9 or (F-32)/1.8	Celsius	°C
		ILLUMINATION		
fc	foot-candles	10.76	lux	lx
fl	foot-Lamberts	3.426	$candela/m^2$	cd/m^2
		FORCE and PRESSURE or STRESS		
lbf	poundforce	4.45	newtons	N
lbf/in^2	poundforce per square inch	6.89	kilopascals	kPa

APPROXIMATE CONVERSIONS FROM SI UNITS

Symbol	When You Know	Multiply By	To Find	Symbol
		LENGTH		
mm	millimeters	0.039	inches	in
m	meters	3.28	feet	ft
m	meters	1.09	yards	yd
km	kilometers	0.621	miles	mi
		AREA		
mm^2	square millimeters	0.0016	square inches	in^2
m^2	square meters	10.764	square feet	ft^2
m^2	square meters	1.195	square yards	yd^2
ha	hectares	2.47	acres	ac
km^2	square kilometers	0.386	square miles	mi^2
		VOLUME		
mL	milliliters	0.034	fluid ounces	fl oz
L	liters	0.264	gallons	gal
m^3	cubic meters	35.314	cubic feet	ft^3
m^3	cubic meters	1.307	cubic yards	yd^3
		MASS		
g	grams	0.035	ounces	oz
kg	kilograms	2.202	pounds	lb
Mg (or "t")	megagrams (or "metric ton")	1.103	short tons (2000 lb)	T
		TEMPERATURE (exact degrees)		
°C	Celsius	1.8C+32	Fahrenheit	°F
		ILLUMINATION		
lx	lux	0.0929	foot-candles	fc
cd/m^2	$candela/m^2$	0.2919	foot-Lamberts	fl
		FORCE and PRESSURE or STRESS		
N	newtons	0.225	poundforce	lbf
kPa	kilopascals	0.145	poundforce per square inch	lbf/in^2

*SI is the symbol for the International System of Units. Appropriate rounding should be made to comply with Section 4 of ASTM E380.

Technical Report Documentation Page

1. Report No.	2. Government Accession No.	3. Recipient's Catalog No.
4. Title and Subtitle **REINFORCED CONCRETE PIPE CRACKS – ACCEPTANCE CRITERIA**		5. Report Date July 1, 2011
		6. Performing Organization Code
7. Author(s) E. Busba, A. Sagüés and G. Mullins		8. Performing Organization Report No.
9. Performing Organization Name and Address Department of Civil and Environmental Engineering University of South Florida (USF) Tampa, FL 33620		10. Work Unit No. (TRAIS)
		11. Contract or Grant No. BDK84 977-06
12. Sponsoring Agency Name and Address Florida Department of Transportation 605 Suwannee St. MS 30 Tallahassee, Florida 32399 (850)414-4615		13. Type of Report and Period Covered Final Report 07/01/2009 - 7/1/2011
		14. Sponsoring Agency Code

15. Supplementary Notes

16. Abstract: Inspection of recently placed reinforced concrete pipes often reveals cracks. Florida DOT was in need of in-place crack acceptance criteria. This project was intended to determine the influential parameters responsible for crack healing in in-place Reinforced Concrete Pipes (RCP), determine what maximum crack width was amenable to autogenous healing and sufficient to mitigate reinforcement corrosion, and formulate guideline models for pipe crack acceptance criteria during construction. A literature survey indicated a reasonable expectation for autogenous healing to eventually occur for cracks narrower than about 0.020 inch. The prognosis was less favorable for wider cracks, and there was little assurance that autogenous healing would reliably take place for crack widths exceeding about 0.100 inch. Laboratory experiments did not produce significant autogenous healing of 0.100-inch or 0.020-inch-wide cracks in reinforced concrete pipe specimens over an approximately 2-month-long period. Corrosion tests showed that significant reinforcement wire corrosion could take place in a short time in reinforced concrete pipe with 0.100-inch-wide cracks, and that corrosion damage was considerably slower when the cracks were 0.020 inch wide. Corrosion was aggravated by the presence of moderate chloride ion contamination (500 ppm), but active steel corrosion occurred even without it. A predictive model for corrosion development in cracked reinforced concrete showed for 500 ppm chloride very short durability projections for the 0.100-inch-wide crack condition, and moderately strong to little limitation in durability for the 0.020-inch-wide crack cases. Acceptable crack width guideline models proposed for discussion included a restrictive alternative, with 0.020 inch width allowable only for environmental chloride no greater than 500 ppm; a less restricted alternative allowing 0.020 inch up to 2000 ppm chloride; and a sliding option for up to 2000 ppm chloride where pipe service life was progressively derated to zero for crack widths increasing from 0.020 inch to 0.100 inch. In all models the acceptable width defaulted to 0.010 inch if the other conditions were not met.

17. Key Words	18. Distribution Statement
Reinforced concrete pipe, cracks, concrete, corrosion, reinforcing steel, autogenous healing	No Restriction This report is available to the public through the NTIS, Springfield, VA 22161

19. Security Classif. (of this report)	20. Security Classif. (of this page)	21. No. of Pages	22. Price
Unclassified	Unclassified	95	

ACKNOWLEDGEMENT

The authors are indebted to the assistance of numerous student participants in the University of South Florida College of Engineering Research Experience for Undergraduates program. Valuable guidance at all stages of the project from the current project manager Larry Ritchie of the State Construction Office and the initial management by Sastry Putcha prior to his retirement are thankfully acknowledged. The assistance of Mario Paredes and Ronald Simmons of the FDOT State Materials Office in conducting cooperative activities is greatly appreciated.

EXECUTIVE SUMMARY

Reinforced concrete pipe is widely used by FDOT in installations requiring service over a period of many decades, so only extremely slow deterioration with time can be accepted. Concrete cracks are often revealed by inspection shortly after placement. A decision must be made then on the part of FDOT as to whether the cracks are of little consequence to future performance and accept the pipe, or if repairs or even pipe replacement is needed. FDOT is in need of in-place crack acceptance criteria. This project had as objectives to:

- Determine the influential parameters responsible for crack healing in in-place Reinforced Concrete Pipes (RCP).

- Determine what may constitute a maximum crack width amenable to autogenous healing and sufficient to mitigate reinforcement corrosion.

- Formulate guideline models detailing pipe crack acceptance criteria during construction.

To achieve those objectives, the investigation consisted of tasks that included a literature and experience review, laboratory experiments, and evaluation of results to formulate a model guideline. The survey showed that few transportation agencies had maximum allowable crack width guidelines for in-place RC drainage pipes. The American Association of State Highway and Transportation Officials, (AASHTO), specifies a maximum in-place width of 0.100 in for non-corrosive conditions and 0.010 in for corrosive conditions. The technical literature indicated a reasonable expectation for autogenous healing to eventually occur for cracks narrower than about 0.020 in. The prognosis was less favorable for wider cracks, and the evidence examined offered little assurance that autogenous healing would reliably take place for crack widths exceeding about 0.100 in.

The laboratory experiments did not produce significant autogenous healing of 0.100-in- or 0.020-in-wide cracks in reinforced concrete pipe specimens over an approximately 2-month-long period. Corrosion tests showed that significant reinforcement wire corrosion could take place in a short time in reinforced concrete pipe with 0.100-in-wide cracks, and that corrosion damage was considerably slower when the cracks were 0.020 in wide. Corrosion was aggravated by the presence of moderate chloride ion contamination (500 ppm), but active steel corrosion occurred even without it. A predictive model for corrosion development in cracked reinforced concrete pipe was formulated and applied to interpret the outcome of the laboratory corrosion tests. For 500 ppm chloride, the overall projection for a loss of wire cross-section failure scenario was corrosion-related durability on the order of several decades for the 0.100-inch-wide cracks, and little limitation (near or above 100 years durability) for the 0.020-in-wide crack cases. A concrete spall failure scenario, deemed to

represent the most adverse corrosion consequences, yielded very short durability projections for the 0.100-in-wide crack condition, and moderately strong to little limitation in durability for the 0.020-in-wide crack cases.

Acceptable crack width guideline models proposed for discussion included a restrictive alternative, with 0.020 in width allowable only for environmental chloride no greater than 500 ppm; a less restricted alternative allowing 0.020 in up to 2000 ppm chloride; and a sliding option for up to 2000 ppm chloride where pipe service life was progressively derated to zero for crack widths increasing from 0.020 in to 0.100 in. In all models the acceptable width defaulted to 0.010 in if the other conditions were not met.

TABLE OF CONTENTS

LIST OF FIGURES

LIST OF TABLES

1 INTRODUCTION

1.1 Project Scope

Reinforced concrete pipes (RCP) are widely used by FDOT in installations requiring service over a period of many decades, so only extremely slow deterioration with time can be accepted. Concrete cracks are often revealed by inspections conducted on recently placed pipes. A decision must be made then on the part of FDOT as to whether the cracks are of little consequence to future performance and accept the pipe, or if repairs or even pipe replacement is needed. FDOT is in need of in-place crack acceptance criteria.

In-place RCP cracks can degrade pipe performance by decreasing structural strength and dimensional stability, permitting leaks and marginally increasing hydraulic resistance, and by allowing premature corrosion of steel reinforcement (Pech-Canul 1999, Sagüés 2001, Sagüés 1989). The latter is of particular concern for long-term performance as it can induce concrete spalls, with potentially severe increase in hydraulic resistance and obstructions as well as loss of load bearing wall thickness. Later stages of reinforcement corrosion would result in additional loss of the strength provided by the reinforcement.

Under certain circumstances concrete cracks can become filled with calcite and similar carbonate deposits from concrete leachates interacting with atmospheric or waterborne CO_2, thus recovering part of the initial strength and resistance to penetration of aggressive substances. That phenomenon, known as autogenous healing (Neville 2002), has been often cited by pipe manufacturers (ACPA 2007) as a process that eventually seals the cracks and prevents the adverse effects indicated above. However, the occurrence of that process cannot be assured (Neville 2002) as it depends on the precise water composition (Neville 2002, Ramm 1998) and flow conditions prevalent at each pipe location. In particular, low pH values retard or prevent healing (Ramm 1998). Moreover, for a given environment, healing is less likely, the wider the crack is (Ramm 1998).

Recent FDOT experience has brought this issue to the forefront. Remote camera inspections in two projects revealed extensive cracking (Sagüés 2008a, 2008b)[1]with apparent widths typically exceeding 0.100 inch in 10% of the instances. Direct inspection of selected locations in one site confirmed the presence of cracks that were long, (e.g., in excess of 50 in), wide (many with largest width exceeding 0.05 in, and one instance reaching 0.3 in) and deep (at least 0.3 in measured with a straight insertion gage, likely much longer due to tortuosity; in one instance the straight gage reached a 2.8 in depth). The depth observations support the expectation that cracks reach down to the reinforcing steel. Site survey data listed

[1] The following restates some prior comments by the author to FDOT in [Sagüés 2008a] and [Sagüés 2008b].

environmental pH values as low as ~ 4.5, which would be highly adverse to autogenous healing (Ramm 1998).

From a durability standpoint, the wider cracks encountered in those cases are of concern due to corrosion of the reinforcing steel wire. At the bottom of such cracks bare steel is likely to be directly exposed to water which, if renewed regularly by flow, would eventually have a pH close to that of the environment. Under neutral and mildly acidic conditions and with natural aeration the steel surface is active, and corrodes where exposed. Galvanic coupling with nearby cathodic steel embedded in the concrete could dramatically aggravate local corrosion of the steel (Kranc 1998) leading to quick section loss and mechanical failure if under tension. The site survey data also showed some locations of elevated chloride content which could further promote corrosion.

Even without aggravating galvanic coupling significant de-rating of performance could take place, given that long term service life requirements, e.g., 100 years, are common in these applications. For example, it might be conservatively assumed that the exposed steel corroded as if it were buried in a typical, not highly aggressive soil environment (with no severe adverse galvanic action). In that case corrosion rate may be expected to be in the order of that used for the durability estimations of the American Association of State Highway and Transportation Officials, (AASHTO), i.e., 12 μm/year (Elias 2000). A typical reinforcing wire ~ ¼ inch (~ 2,500 μm) in diameter and roughly uniform corrosion around the perimeter may be considered. There, a penetration to ~ 1/3 of the radius (corresponding to ~ 1/2 cross-section loss and hence risking fracture if the loads on the pipe are near design capacity) would be reached after only about 40 years of service. If aggravating galvanic coupling were to be present as well, the derating would be proportionately more severe (Kranc 1998) conceivably resulting in some failures after service times in the order of one decade or so. Increased severity from, for example, elevated chloride content could further decrease durability. It is noted also that if corroded wires would fail, the initial cracks could open further leading to more exposed steel, further corrosion and potential concrete spalling.

FDOT at present has acceptance criteria for pipe cracks observed before placement in Section 449, Item 449-4.1 of its Standard Specifications for Road and Bridge Construction (FDOT 2010) effectively rejecting RCP that show cracks having width above 0.01 in and extending for a length of 12 in or more, which is as specified in ASTM Standard Specification C 76. The Department also relies on the American Society for Testing and Materials ASTM C 76 standard and AASHTO LRFD Chpt. 27 guidance for crack observation and acceptance or rejection once the pipe is in place, where static and dynamic stresses during and after placement caused the wide cracks noted earlier. Because of the interplay between aggravating (such as promoting corrosion related damage) and mitigating (autogenous healing) factors, it is not clear at present what may be considered to be an acceptable crack width and under which environmental composition circumstances.

1.2 Project Objectives and Research Tasks

Based on the needs indicated in the previous section, the present investigation was conducted with the following main objectives:

(1) Determine the influential parameters responsible for crack healing in in-place RCP.

(2) Determine what may constitute a maximum crack width amenable to autogenous healing and sufficient to mitigate reinforcement corrosion.

(3) Formulate guideline models detailing pipe crack acceptance criteria during construction.

To achieve those objectives the investigation consisted of tasks that included a literature and experience review, laboratory experiments, and evaluation of results to formulate a model guideline.

Consistent with the resources available, the literature / experience review task was the main source of information for achieving the project objectives. Whenever identifiable, current guidelines for allowable in-place pipe crack acceptance criteria stated by U.S. State DOTs and Federal agencies, as well as in relevant foreign specifications and technical literature on the subject were reviewed and discussed with FDOT stakeholders. The information was used to adjust the scope of the remaining tasks and to aid in establishing final recommendations.

The laboratory investigation task was conducted to obtain supplemental indication of the extent of pipe deterioration that could result from reinforcement corrosion induced at pipe cracks, as well as on the extent of possible autogenous healing. Samples of RC pipes from two different pipe manufacturers were evaluated. The samples had two different crack sizes and were exposed to natural waters representative of anticipated field conditions. The resulting corrosion was quantified, and a corrosion predictive model was developed to project service life impact as function of crack size. Healing tendency was evaluated to the extent feasible under the test conditions.

In the evaluation task the outcome of the previous activities was integrated and analyzed to propose a set of guidelines for consideration by the Department for allowable crack size.

2 LITERATURE / EXPERIENCE REVIEW [2]

Agency specifications and literature sources have been reviewed. Relevant findings are described under headings of individual sources flagged by bullets. Full literature citation for each source is given in the References chapter. The sources include a survey conducted by FDOT seeking information on existing relevant specifications by other state and federal agencies. The sources also include relevant studies and specifications by other national and international organizations, in addition to sources from the open technical literature.

2.1 Existing Standards by State and Federal Agencies

- **FDOT survey result for in-place RC pipe cracks based on (FDOT 2009)**

The FDOT State Materials Office conducted a nationwide survey to explore any identifiable existing State / User agency standards. The survey questions were essentially:

1) Does your agency currently have a specification for maximum crack width in *installed* highway drainage pipe?

If answer to (1) is yes, please provide the information.

If answer to (1) is negative but other measures or criteria beyond those in current ASTM standards are in place to limit crack development in installed pipe, please provide pertinent specification information.

2) Does your agency currently have any specifications for the type of concrete to be used in RC pipe supplementing those in ASTM C 76, C 655?

3) Do your current agency specifications explicitly take into account the development of autogenous healing as a mitigating factor of the effects of concrete cracking?

The survey results are indicated in Table 2.1.

[2] Review of the material discussed in this chapter often includes paraphrasing and direct quotes, some of them redacted, from the publications examined. For readability, quotation marks have been inserted only in the more extensive excerpts.

Table (2.1) Results of a survey on existing crack criteria adopted by other State DOTs

DOT	Criteria for max. crack width for installed RC pipes		Criteria for max. crack other than 0.01 inch of ASTM C76		Specification for type of concrete to be used in RC pipes		Specifying autogenous healing as a mitigation factor	
	Yes	No	Yes	NO	Yes+	No	Yes	No
20 State DOTs	4	16	2	18	8	12	0	20
Ohio*	0.100 in							
Pennsylvania	0.007 in							
Georgia	Reject pipes having: through-wall cracks of any dimension/ damage to pipe ends affecting joints/ 0.01" of 1 foot or longer							
Caltrans	0.010 in corrosive (pH < 5.5 & Chloride > 500 ppm) / 0.100 in non corrosive							

* Ohio DOT made a reference to their document # SS802 which indicates that no action would be required up to 0.075" crack width

+ Most DOTs adopt AASHTO M170

- **Ohio DOT (2008):** Ohio DOT adopted the "Supplemental Specification 802, Post Construction Inspection of Storm Sewers and Drainage Structures, April 15, 2005, supplemental to Construction and Material Specifications, 2008. The specification, in section 802.10, Table 802.10. A, calls for a crack width of 0.075 in maximum. The specification is based on OCPA, Ontario Concrete Pipe Association documentation discussed elsewhere in this chapter (OCPA 2000).

- **Caltrans (2009):** The California DOT adopted the AASHTO specification described elsewhere in this chapter (AASHTO 2006) 0.100 in maximum width except for more corrosive environments, as indicated in their Construction Manual, chapter 4, section 65-Reinforced Concrete Pipe (Caltrans 2009).

2.2 Studies and Specifications by Other Agencies

2.2.1 User Agencies

- **AASHTO (2006):**

  AASHTO specification allows for a crack width of 0.1 in maximum in conditions specified as less aggressive (pH = 5.5 or greater; Chloride concentration = 500 ppm or less), and 0.01 in maximum in more corrosive environments. The specs are based on the report "Diamond Bar Culvert, A study of corrosion of the steel reinforcement relative to crack widths in reinforced concrete pipe", prepared by the technical committee of the California Precast Concrete Association, February,1976. The study indicated that examination of cracks disclosed no evidence of autogenous healing but no corrosion of steel reinforcement was observed at crack widths up to 0.100 in for less aggressive environments where slabbing of the pipe wall had not occurred. The study however calls for further investigations to study crack/corrosion/serviceability relationships.

- **Parks (2008):** The American Water Works Association sponsored a lab experimental study and published a report on autogenous healing of concrete in the drinking water industry. The report main findings are:

  - Healing, in some test specimens, resulted in substantial strength development in pH 9.5 water with high levels of magnesium and silicon, whereas in other specimens no strength gain was observed.

  - Traditional scaling indices such as Langelier index are not reliable to predict if appreciable amount of autogenous healing of cracks in concrete will occur.

  - Age of concrete may play a role in impeding or enhancing autogenous healing.

  - Chloride diffusion rates were reduced by autogenous healing although did not return to original levels of uncracked concrete.

  - Stagnant water conditions may increase pH, leading to higher levels of autogenous healing and this may not be the case in flowing water conditions.

- **AWWA (2007):** The American Water Works Association adopted a standard, C205, for shop-applied cement mortar protective lining and coating for steel water pipe-4 inches and larger. While this standard does not apply directly to

reinforced concrete pipe, it is mentioned here as it is of interest. The standard, in its section (4.4.6.2) states the following:

- Lining cracks up to 1/16 inch (1.6 mm) in width need no repair.
- Lining cracks greater than 1/16 in need no repair if it can be demonstrated that autogenous healing is possible under continuous soaking in water.
- Hairline coating cracks need no repair. Autogenous healing is not expected on pipe exterior.

- **AWWA (1999):** The American Water Works Association adopted standard, C301, for pre-stressed concrete pipes. While this standard does not apply directly to reinforced concrete pipe, it is mentioned here as it is of interest. The standard states the following:
  - Interior concrete core surface - circumferential cracks or helical cracks having a width of 0.06 in (1.5mm) or less are acceptable without repair.
  - Cracks having width greater than 0.06 in (1.5 mm) are acceptable without repair if it can be demonstrated that they can autogenously heal.
  - No visible cracks longer than 6 in (150mm) are permitted.
  - Exterior mortar coating surface shall be free of visible cracking over pressurized zones (That does not apply to surface crazing of widths that cannot be measured).
  - Over non-pressurized zones of the pipe, exterior cracks in mortar coating up to 0.01 in (0.25 mm) are acceptable without repair.
  - Cracks greater than 0.01 in shall be repaired by rubbing with wet cement paste or filling with neat cement slurry.

- **GMRA (2007):** A study by the Great Man-Made River Authority summarized various International standards, Table 2.2. The study described that the standards are conflicting on maximum allowable crack widths for cement mortar lining of steel and ductile iron pipes. Figure 2.1 shows the results of a field investigation of autogenous healing of concrete cracks. Summary of the results of a field study, conducted by GMRA, are given below:

Table (2.2) Various international guidelines on allowable crack widths for mortar lining of steel and ductile iron pipes [GMRA 2007]

Standard / CoP	Relevant Dia	Drinking Water	Aggressive Water	Comments
BS EN 10298 [12]	all	< 1.5 mm	< 0.5 mm	Allows larger cracks to be pre-treated by exposure to drinking water to allow the cracks to partially heal down to acceptable level. Where cracks do not reduced to required width then repair required Capability of CML to heal is decreased when stored for long periods in moist atmospheric conditions.
BS EN 545 [24]	< 2000 mm Ø	< 0.8 mm		As measured in dry condition.
BS ISO 4179 [16]	≥ 2200 mm Ø	< 1.5 mm	< 0.8 mm	Allows "hollow sounds"
AWWA A21.4 [25]	> 610 mm Ø	No width limit		Larger cracks acceptable if it can be demonstrated that they will heal autogenously on prolonged exposure to water. Curing period should be limited to 7 days. Excessive number of cracks / dummy areas considered to be defect areas (however, see note below)
AWWA C602 [1]	> 100 mm Ø	< 1.6 mm		
BS 534 [26]	all	< 0.25 mm	< 0.25 mm	Crack width as measured under "saturated" conditions. Crack length < 300 mm
WRc [13]	all	< 2 mm	nc	

- Calcium carbonate precipitation potential (CCPP) is a better indicator of autogenous healing than traditional scaling indices (Langelier and Ryznar indices)
- A value of CCPP greater than 5 mg/L ($CaCO_3$) would have sufficient material to allow healing to occur.
- Maximum crack that can heal depends on water chemistry and age of concrete/mortar.
- Full closure of cracks in several weeks in fully saturated condition.
- When pipes are left dry for extended periods, healed existing cracks are likely to re-open but new cracks are unlikely.
- Cracks of 0.078 in (2mm) widths completely healed after 25 days in fully submerged condition.

- Cracks sealed by a combination of both mortar swelling and autogenous healing.

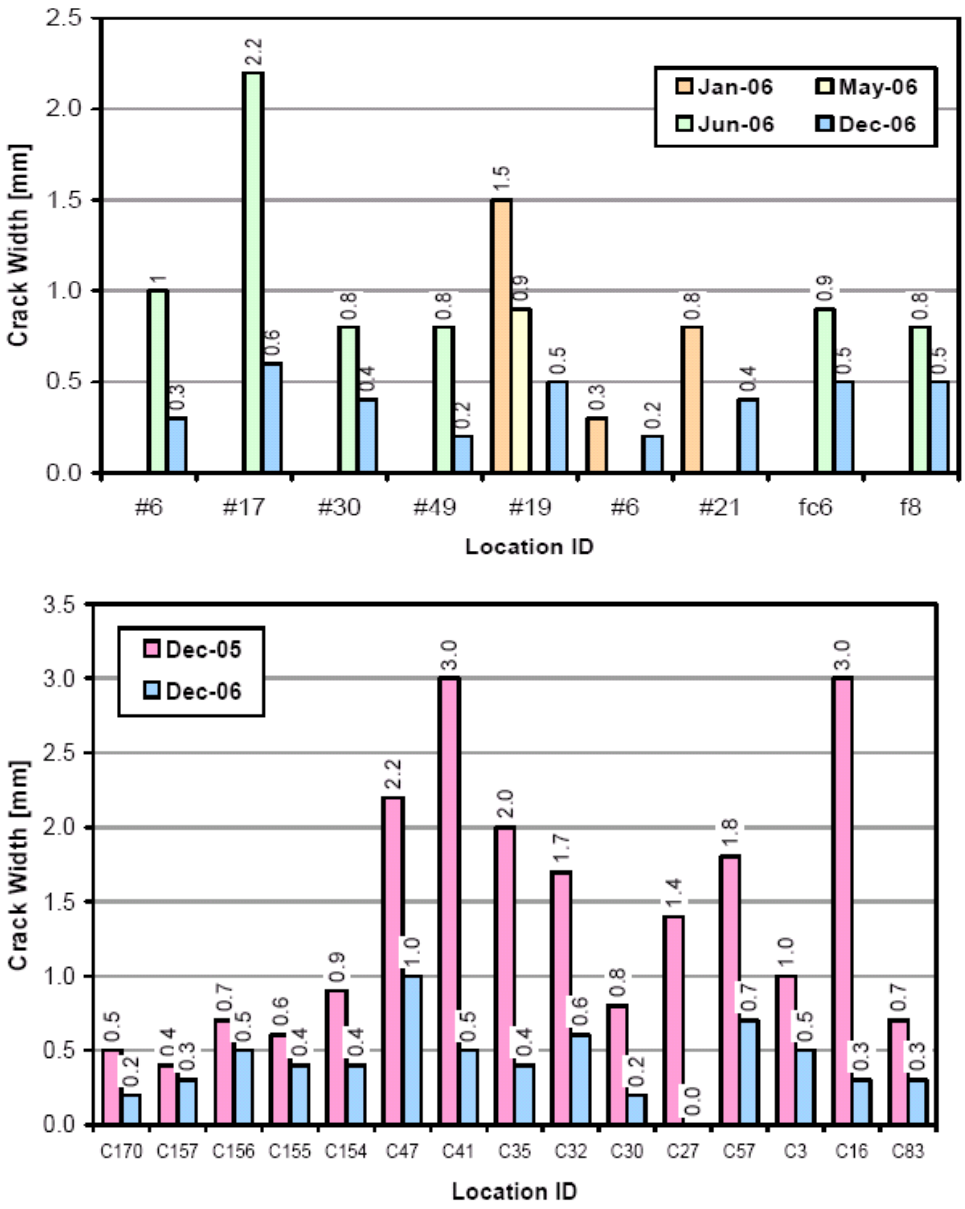

Figure (2.1) Reduction in crack width due to autogenous healing of interior cracks in cement-mortar-lined ductile iron pipes [GMRA 2007]

2.2.2 Producer Agencies

- **ACPA (2007a):** The American Concrete Pipe Association reported that professor M.G. Spangler noted his opinion on RCP cracks as “cracks up to 1/16 inch in width will not permit corrosion except under the most adverse conditions”. The association also reported that RC pipes with 0.02 in maximum wide cracks that are not penetrating the pipe wall and having at least 1 in concrete cover would provide the same durability as uncracked pipes in aggressive environments.

- **ACPA (2007b):** The American Concrete Pipe Association reported, in an article on effects of cracks in reinforced concrete sanitary sewer pipe, the findings of a study authorized by Texas Concrete Works in March 1971as summarized below:
  - There is little or no probability of deterioration of reinforcing steel with a 2 in concrete cover exposed by a hairline crack, even when sulfuric acid is present.
  - Concrete pipe has a high probability of incurring Autogenous Healing of cracks if any moisture is present either on the inside or outside of the pipe.

- **ACPA (2007c):** Based on a study on the effect of cracks in culvert RCP, reported by the Technical committee of the California Precast concrete pipe association in the February, 1976, report “Diamond bar culvert: a study of corrosion of steel reinforcement relative to crack widths in RC pipes" (results in Table 2.3) , the American Concrete Pipe Association reported that:
  - Cracks substantially larger than 0.01 in did not significantly affect the structural integrity of the pipe.
  - Corrosion was not observed up to crack widths of 0.100 in. Structural integrity was not affected by cracks up to 0.100 in where slabbing failure has not occurred. Life expectancy was not affected.
  - Concrete encasement of culverts was not necessary to maintain structural integrity even with crack width of 0.2 in.
  - In areas where slabbing failure occurred and no epoxy grouting performed, corrosion was observed. However corrosion rate would lead to

life expectancy of several hundred years. This is based on a linear projection of observed corrosion, unchanged environmental conditions and reinforcing steel with ultimate working stress up to 2.

- No evidence of autogenous healing was observed.

Table (2.3) Results of Field study of cracked RC pipes [ACPA 2007c]

Pipe No.	Core No.	Location	Crack Width (In.)	Concrete Cover (In.)	Wall Thickness	Comments
22	1	Springline	.060	1-1/4	6-5/8	Circumferential crack extended into steel. No corrosion.
	2	Invert	.160	1	6-1/2	Epoxy grout to depth of 2-1/2". Concrete slabbed. Light corrosion.
23	3	Invert	.200	1-1/8	6-5/8	Epoxy grout to depth of 2-1/2" extending 6" into vertical crack. Concrete slabbed. Light corrosion.
29	4	Invert	.110	1-1/8	6-5/8	Epoxy grout to depth of 4". Concrete slabbed. Light corrosion.
	5	Springline	None	1-1/4	6	No cracks. No corrosion.
30	6	Invert	.140	3/4	6-3/8	Epoxy grout to depth of 2-7/8". Concrete slabbed. Moderate corrosion to deformations.
34	7	Invert	Crack covered w/ epoxy	1-3/4	6-1/2	Epoxy did not penetrate below surface. Concrete slabbed. Moderate corrosion to deformations.
34	8	Springline	None	1-1/4	6-1/4	No cracks. No corrosion.
48	9	Crown	.030	1-5/16	6-1/4	Crack extends into rebar. No corrosion.
56	10	Invert	.100	1-1/4	6	Crack extends into rebar. No slabbing. No corrosion.
65	11	Crown	.025	2-3/8	6-1/2	Crack feathers out at rebar. No corrosion.
21	12	Invert	.090	1-1/8	7-3/8	No epoxy repairs. Slabbing of concrete under rebar. Moderate corrosion.
	13	Crown	.020	3-3/4	7-1/2	Crack extends to rebar. No corrosion.
	14	Springline	None	1-3/8	7-1/2	No corrosion.
	15	Invert-30". downstream	.060	1-1/8	7-1/2	Slabbing under rebar.
	16	Invert-13". downstream	.015	1-1/8	7-3/8	No slabbing. No corrosion.

- **OCPA (2000):** The Ontario Concrete Pipe Association stated in its Concrete Pipe Design Manual that RC pipes with up to 0.01 in wide cracks are acceptable in aggressive environments and calls for consideration to be given to 0.02-in crack width.

- **CPAA (2004):** The Concrete Pipe Association of Australasia reported the following technical literature review results:

  - Carbon dioxide dissolved in low concentration from atmosphere plays a role in the healing process, precipitating calcium carbonate, but not necessarily to initially dissolve calcium from the cement.

  - Autogenous healing will take place in blended cement even though such concrete may be found not to contain any free lime.

  - Roberts (Ref. 5 cited in CPAA 2004) confirms that the type of water and the cementitious material have minimal effect.

  - Mohammed (Ref. 8 cited in CPAA 2004) investigated autogenous healing in a marine environment and found that cracks of width less than or equal to 0.5 mm (0.0196 in) healed before any significant effect on steel rebar.

  - Beeby (Ref. 6 cited in CPAA 2004) reported on concrete beams loaded to create crack widths up to 0.4 mm and exposed to marine environment. The beams were broken open after 1, 2, 4 &10 years. The extent of corrosion was less in the finer cracks at the ages of 1 and 2 years. After ten years the remaining difference was small due to autogenous healing.

- **McGuire (2004):** The practice of the Concrete Pipe Association of Australasia (CPAA) is that up to 0.5 mm (0.0196”) circumferential cracks and / or 0.15 mm (0.005”) longitudinal cracks are acceptable in RC pipes with 25 mm (1 in) concrete cover, as stated in Table 2.4.

Table (2.4) Crack criteria of CPAA [McGuire 2004]

Defect	Description	Magnitude	Solution
Type 1	Circumferential crack	Width <0.15 mm	Accept
	Longitudinal crack	Width <0.15 mm	Accept
Type 2	Circumferential crack	0.15 mm< width <0.50 mm	Accept
	Longitudinal crack	Width >0.15 mm	Assess design
Type 3	Circumferential crack	Width >0.50 mm	Assess implication of ingress
	Longitudinal crack	Width >0.50 mm	As per Type 2
Type 4	Chip or spall	Depth <0.25×cover	Accept
Type 5 or 6	Chip or spall	Depth >0.25×cover	Assess implication Repair

- **CPAA (2008 a):** The Concrete Pipe Association of Australasia (CPAA) issued in this document engineering assessment and acceptance guidelines for in-place circumferential cracking in RC pipes as shown in Table 2.5

Table (2.5) CPAA acceptance guidelines for circumferential cracks in RC pipes [CPAA 2008a]

Size of crack	Action recommended
< 0.15 mm	No action required
0.15 mm to 0.5 mm	No action required, allow autogenous healing to take place
0.5 mm to 1.0 mm	Monitor and allow autogenous healing and review after 12 months
1.0 mm to 2.0 mm	Assess potential for fines to migrate through crack (which may degrade the bedding)
2.0 mm >	Crack likely to be all way around and may require repair or replacement of pipe

- **CPAA (2008 b):** The Concrete Pipe Association of Australasia (CPAA) issued in this document engineering assessment and acceptance guidelines for in-place longitudinal cracking in RC pipes as shown in Table 2.6

Table (2.6) CPAA acceptance guidelines for longitudinal cracks in RC pipes [CPAA 2008b]

For pipes with longitudinal cracks - top and bottom	
Size of crack	**Action recommended**
< 0.15 mm	No action required - crack unlikely to extend through the wall and equivalent to the design serviceability load crack defined by AS/ NZS4058.
0.15 mm to 0.5 mm	Monitor for stability of crack. Cracks up to 0.5 mm are not considered to be a durability risk. If crack is stable, no further action required.
0.5 mm >	Engineering assessment required to consider effects of long term loads.
For pipes with longitudinal cracks - sides	
< 0.15 mm	No action required. If pipe is in final loaded condition, the imposed loads will close longitudinal cracks in the spring zone.
0.15 mm >	Engineering assessment required. Repair may be deferred to allow autogenous healing to occur. If after agreed monitoring period autogenous healing has not occurred refer to recommended repair methods for action.

2.3 Other Technical Literature

2.3.1 Review Articles on Factors Promoting Autogenous Healing

- **Neville (2002):** An extensive state-of-the-art review was conducted on the process of autogenous healing in concrete. The main findings are summarized below. Literature sources not referenced in this report can be found in Neville (2002).

    - Healing can take place only in the presence of water. Full contact of the crack surfaces with water is essential.

    - There are two possibilities of autogenous healing: Formation of calcium hydroxide (in very young concrete only) and formation of calcium carbonate later on. The latter requires, in addition to water, the presence of carbon dioxide.

    - Silting of cracks or deposition of debris can contribute to healing but cannot provide it by itself.

    - The crack will remain “as is” in dry conditions especially where cracks result from drying shrinkage.

- Temperature changes contribute to the closing of cracks. There are examples of pipes put into service to carry water at a much lower temperature than the previous air temperature. The resulting thermal contraction had a positive effect on closing the cracks.
- Generalizations about the maximum width of cracks that will heal are not possible.
- Above a certain width adequate autogenous healing will not take place. Also beyond a period of about 3 months, significant healing stops.
- The strength of healed concrete is rarely of interest and has not often been determined.
- Access of water and oxygen to steel at the bottom of crack will not automatically lead to corrosion unless there is sufficient supply of oxygen to the portion of steel covered by mortar.
- Information deduced from lab experiments is difficult to translate into practical situations due to little knowledge of crack widths and other conditions in real life.

The following is a summary of some of the findings of other researchers cited in the Neville study:

- Hearn (Ref.3 cited in Neville 2002)
  - Autogenous healing is due to further hydration of cement and formation of calcium hydroxide and due to formation of calcium carbonate.
- Lauer and Slate (Ref.4 cited in Neville 2002)
  - The presence of calcium carbonate is due to the reaction of carbon dioxide in ambient water or air with calcium hydroxide present at the crack surface.
  - Even when the RH was 95% the extent of healing was much lower than in water.
  - Periodic wetting without periods of low RH in between results in the healing process but may not produce full closure of cracks.
  - The development of strength is a function of the extent of complete bridging of the crack and of the proportion of the volume of the crack that has become filled by the new compounds.

- Wagner (Ref.5 cited in Neville 2002)

- The crack filler consists of calcium carbonate.

- In pipes, autogenous healing may be supplemented by the expansion of the mortar lining owing to the absorption of water into the previously dried concrete.

- Cracks up to 0.03 in wide sealed by autogenous healing after 5 years. One crack of 0.06 in wide became sealed.

- Clear (Ref.1 cited in Neville 2002)

- The formation of calcium carbonate is significant in later stages of exposure of cracks to water but this mechanism is not predominant in the first few days.

- Gautefall and Vennesland (Ref.8 cited in Neville 2002)

- Silica fume in the mixture had no influence on autogenous healing.

- In specimens immersed in sea water, cracks more than 0.024 in wide were susceptible to corrosion attack but this did not happen when the cracks were less than 0.016 in wide.

- Products of corrosion of steel may contribute to blocking of cracks.

- Loving (Ref.10 cited in Neville 2002)

- Shrinkage cracks of 0.03 in to 0.06 in wide, in (5 to 8 ft) RC pipe, completely closed by autogenous healing in service after 5 years.

- Lea (Ref.11 cited in Neville 2002)

- Provided the width at the surface is not more than about 0.008 in, the presence of such cracks does not usually lead to progressive corrosion of the steel, though the critical width depends on concrete cover and exposure conditions.

- Ngab (Ref.13 cited in Neville 2002)

- A condition necessary for a successful recovery of strength through autogenous healing is that there is no longitudinal displacement of concrete on the opposite sides of a crack “fit”.

- Sustained compression across the planes of the crack enhances the process of healing.

- Venessland and Gjorv (Ref.15 cited in Neville 2002)

- In specimens immersed in sea water, corrosion of the exposed steel in the crack was a function of the ratio of the area of the cathode to the area of the anode.

- Although corrosion was observed for all crack widths 0.016 in or more, corrosion damage never developed in the 0.02-in cracks in spite of the galvanic coupling.

- For crack widths smaller than 0.016 to 0.02 in, precipitation of reaction products may effectively clog up the crack and thereby inhibit the corrosion before any damage to the steel has occurred.

- Jacobsen (Ref.12 cited Neville 2002)

- Healing resulted in about 1/3 reduction in chloride ion migration.

- **Edvardsen (1999)** (also cited in Neville 2002)

  - Calcium carbonate is almost the sole cause of autogenous healing.

  - Water hardness and concrete composition do not seem to have influence on the process of autogenous healing nor does the value of pH.

  - In an experiment involving through thickness cracks, up to 50% of the cracks having 0.08 in wide healed completely after 7 weeks of water exposure. The proportion of cracks closed depended on the water pressure.

- **Ramm (1998)**

This investigation established that autogenous healing was less efficient with water pH < 5.2. Extensive leaking took place when cracks were wider than ~ 0.016 in; at pH 5.2 leaking was significant even when crack width was as small as 0.008 in.

2.3.2 Articles on Relationship between Corrosion and Concrete Cracks

- **Tarek Uddin (2003a):**

  - Macrocell corrosion of steel between cracked and uncracked regions is significantly influenced by W/C ratio.

- Narrow cracks healed in long-term marine exposure irrespective of cement type.

- **Tarek Uddin (2003b):**
  - Autogenous healing prevented corrosion of steel in a concrete joint (that acts like a crack) exposed to a marine environment.
  - Microcell corrosion at concrete joint regions was not higher than other regions.
  - Joint portion does not necessarily act as an anodic region.

- **Torres (2004):**
  - In reinforcing steel, the corrosion penetration depth required to cause the surrounding concrete to crack (Xcrit) is greater in the case of localized corrosion.
  - The value of X critical increased as relative humidity increased
  - On first approximation corrosion rate had no effect on the value of Xcrit.

- **Vidal (2004):**
  - A model is presented to predict critical rebar cross-section loss required for concrete cover cracking based on 14-year experiment. The formula given by Eq (2.1) is function of concrete cover-diameter ratio, original rebar cross-section and the pit concentration factor.

$$\Delta A_{s0} = A_s \left[1 - \left[1 - \frac{\alpha}{\phi_0} \left(7.53 + 9.32 \frac{C}{\phi_0} \right) 10^{-3} \right]^2 \right] \qquad \text{Eq. (2.1)}$$

    Where ΔA_{s0} is critical loss in cross-section in mm^2; A_s is original rebar cross-section in mm^2; C is concrete cover in mm; Φ_0 is original rebar diameter in mm and α is the pit concentration factor (8 for localized corrosion attack induced by chloride).

  - Another linear relationship Eq (2.2) relating rebar cross-section loss to crack width was proposed (function of critical rebar cross-section loss).

$$W = K(\Delta A_s - \Delta A_{s0}) \qquad \text{Eq. (2.2)}$$

    Where W is crack width in mm; ΔA_s is loss of rebar cross-sectional area and K = 0.0575

- For different rebar diameters, the same penetration loss may result in different cross-section loss.
- Crack initiation depends on cover - diameter ratio and rebar diameter while crack propagation does not (it depends on cross-section loss).

- **Alonso (1998):**

  - In the case of higher corrosion rate, corrosion penetration depth(X) required for a concrete crack to reach a certain crack width is greater (Crack propagation). Corrosion rate is less significant on Xcrit (Crack initiation, i.e., crack width = 0.05 mm). This effect may be due to different types of oxide formed at different corrosion rates. The effect on Xcrit becomes significant when the concrete cover is greater.
  - The higher the water-to-cement ratio (porosity) the higher the values of Xcrit and X for a certain crack width.
  - Increasing cover to diameter ratio C/d increases Xcrit and X. (For general corrosion Xcrit is about 50 microns for the cases where C/d ratio were greater than 2).
  - Higher Xcrit needed for top cast rebars.
  - A linear relationship for propagation of the type W = a + bX. For initiation Xcrit = 7.53+9.32C/d. In the second part of propagation stage a less slope is observed. More time is needed to reach a certain width (may be due to available path for corrosion product to diffuse out).

- **Sahmaran (2007) :**

  - The relation between effective chloride diffusion coefficient and crack width is a power function.
  - The effect of crack width on effective diffusion is significant for crack widths higher than 135 micrometer (0.005”).
  - Significant amount of self-healing was observed for crack widths less than 50 micrometer (0.002”).

- **Jaffer (2008):**

  - Corrosion occurred at intersection of rebars with cracks.
  - Cracked high performance concrete was more protective than ordinary Portland cement concrete.
  - The type of loading had less impact on corrosion than the type of concrete and exposure conditions.

- **Yang (2009):**

  - Engineered fiber-reinforced cementitious composites were investigated.
  - For those materials crack widths needed to be <150 μm (~0.006 in) for noticeable self-healing.

2.4 Overall Observations

Various agencies and organizations specify different values for maximum allowable crack width for in-place RC drainage pipes. AASHTO specifies a maximum in place width of 0.100 in, but only under non corrosive conditions. The AASHTO limit decreases to 0.010 in for corrosive conditions. The AASHTO 0.100 in limit value for non-corrosive conditions seems based largely on an investigation (AASHTO 2006 and Table 2.2) where no autogenous healing had been documented but no reports of corrosion had taken place either. Concern may exist as to that limit being not conservative enough. On the other hand, the 0.010 in value for more corrosive environments appears to be a possibly overly conservative limit, possibly influenced by the strength test limit in ASTM C76 (ASTM 2011), which is intended for that test but not as a criterion for field performance. If conditions leading to autogenous healing were present, some corrosion resistance would be expected result and cracks wider than 0.010 in could be permissible. Independent laboratory investigations reviewed here tended to report efficient autogenous healing, or absence of severe corrosion, when crack widths did not exceed about 0.020 in, so a value in that order may represent a possibly less overly conservative alternative to the 0.010 in the AASHTO limit for other than very mild environments. Indeed, acceptable crack widths of 0.002 in are stated in CPAA (2008 a, 2008 b) as well as OCPA (2000). It is noted however that those values are proposed by pipe producer associations and not by users.

Given the above considerations, the experiments, described in the next chapter, were conducted to examine two crack width conditions, 0.020 in and 0.100 in, with pipe materials currently used by FDOT. The objective was to obtain supplemental information on the extent of autogenous healing and corrosion damage that may result in both cases, and apply the findings together with those from the literature review toward consideration for establishing an FDOT permissible in-place crack width guideline.

3 INVESTIGATION METHODOLOGY[3]

3.1 General Experimental Approach

RC pipes from two different pipe manufacturers were evaluated for the possible extent of reinforcement corrosion at preexisting cracks in a moderately aggressive simulated natural water environment. For the evaluations, specimens cut out of the pipes were cracked to obtain narrow (0.020 in) and wide (0.100 in) openings, representing the limits of variation encountered in the literature review for the maximum acceptable crack sizes reported by various researchers and / or organizations. Uncracked specimens served as controls. Initially the tests were to be conducted with and without prior development of autogenous crack healing, so as to establish whether the latter provided a substantial benefit in preventing or delaying onset of corrosion. However, exploratory procedures failed to produce significant autogenous healing in the laboratory specimens within the allotted time for the project. Consequently, all corrosion experiments were conducted only for the case of unhealed preexisting cracks. Experiments aimed to promote autogenous healing were nevertheless continued throughout the rest of the project to provide additional background information.

3.2 Products Selected for Evaluation

The reinforced concrete pipe products from each of the two manufacturers were designated by the code names R-Type and Z-Type respectively. Each manufacturer provided two pipes from their regular production to the FDOT State Materials Office laboratories. There the pipes were sectioned into test specimens (quadrants) according to a plan provided by the University of South Florida (USF). The test specimens were identified, labeled and delivered to USF for laboratory testing.

Each manufacturer provided Class III B-Wall (2" wall) 8 ft x 18 in RC pipes in duplicate (4 pipes total). The products were manufactured in accordance with ASTM C76 (ASTM 2011). Product data provided by the manufacturers is listed in Table 3.1 and 3.2 below. The R-Type concrete mix contains fly ash whereas that of Z-Type has not but includes higher cement content. Such differences are illustrative of the variety of materials encountered in the supply to FDOT projects, which may, in turn, diversify healing potential and corrosion behavior.

[3] Crack widths reported hereafter as 0.020 in or 0.100 in are given in that manner to facilitate visual conversion into thousands on an inch (20 and 100 respectively). That designation does not necessarily represent numeric accuracy to the third significant figure beyond the period.

Table (3.1) Mixture proportions of the R-Type and Z-Type pipes as reported by manufacturers

Mix design 4000 PSI			
Material Type	**Material Quantity**		**Unit**
	R	**Z**	
Cement	391	590	Lb/yd^3
Fly ash	103	0	Lb/yd^3
sand	1689	1895	Lb/yd^3
stone	1773	1300	Lb/yd^3
water	16	29	Gal/yd^3
Admixture	0	0	Oz

Table (3.2) RC culvert pipe general specifications as reported by manufacturers

Type	**R**	**Z**
Pipe Age (Cast Date)	3/11/2010	2/18/2010
Concrete Mix Composition	Mfr. Mix Design Designation:4000 PSI	Mfr. Mix Design Designation: No. 1
Class of Pipe	Class III B-Wall (2.5 in Wall)	Class III B-Wall (2.5 in Wall)
Interior Concrete Cover (nominal)	1 in	1 in
Pipe Dimensions	8ft long X 18 inch in diameter	8ft long X 18 inch in diameter
Dimension and Spec of Reinforcing Steel in^2/linear ft of pipe wall	0.07 wire bell steel area, 0.07 steel area for wall steel; ASTM C76, FDOT Design Standards Section Index #280, ASTM C478	0.07 wire bell steel area, 0.07 steel area for wall steel; ASTM C76, FDOT Design Standards Section Index #280, ASTM C478

3.2.1 RC Culvert Pipe Sectioning

RC culvert pipe test specimens were prepared by sectioning each pipe as illustrated in Figure 3.1 to produce 8 quadrants from each pipe with a total of 32 quadrants from the four pipes. The two pipes from each manufacturer were identified as A and B. Two concrete pipe sections (rings) were extracted from each pipe and labeled as 1 and 2. Specimens identification was performed to facilitate traceability in terms of pipe type (R or Z), pipe ID character (A or B), and pipe section (concrete ring) number (1 or 2) and cutting clock positions (0 to 360^o) looking from the spigot end side and based on a selected reference as the zero degree line. Quadrants were also marked with arrows to indicate specimen sides facing the bell and spigot ends of the pipe.

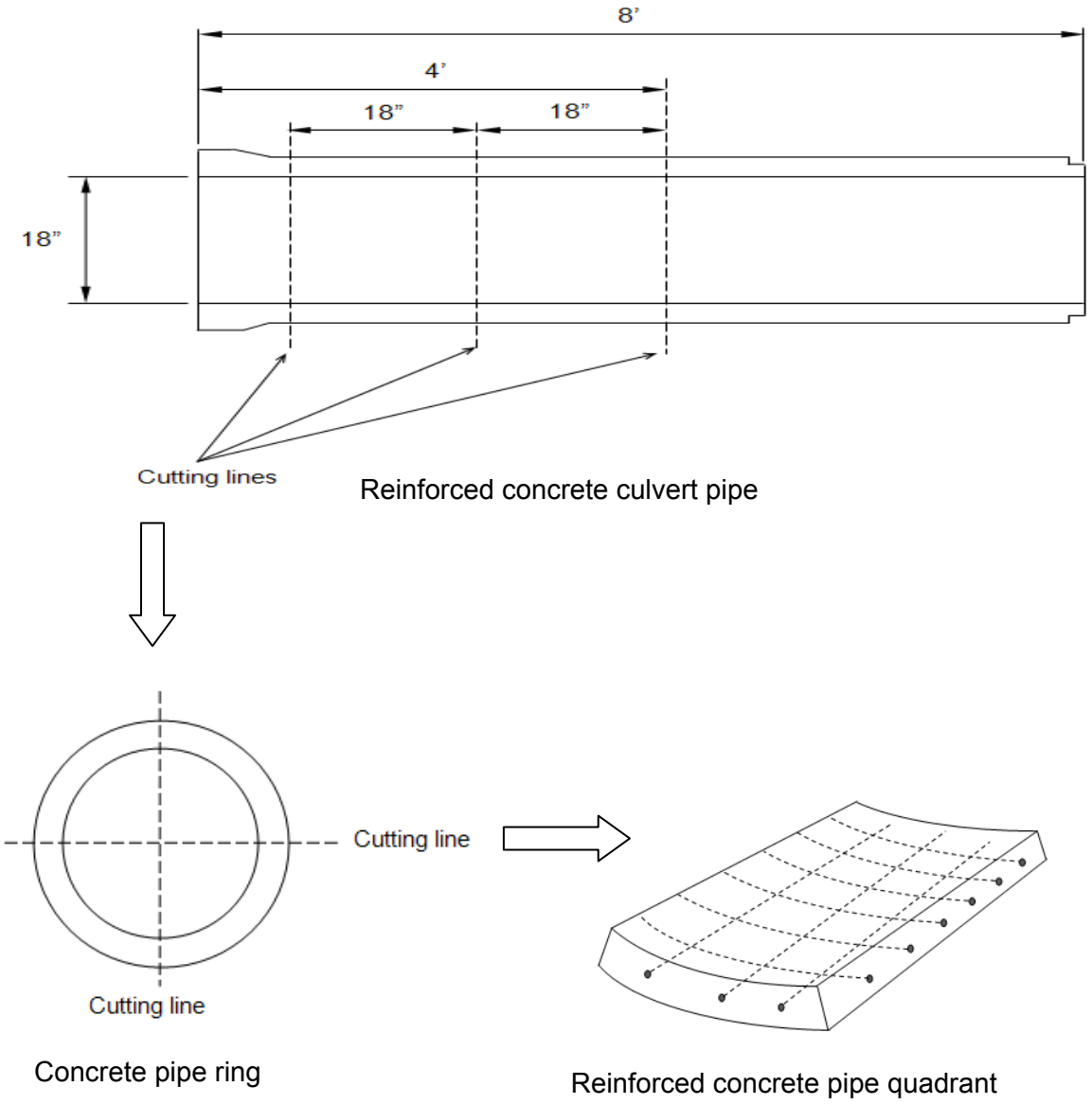

Figure (3.1) A reinforced concrete culvert pipe Sectioned to produce 8 quadrants

The specimens were labeled (R1 to R14, RA & RB) and (Z1 to Z14, ZA & ZB). Four specimens, two of each type, were used for preliminary testing. Table 3.3 cross-references each specimen with the original FDOT identification for traceability purposes. Appearance is illustrated in Figure 3.2.

Table (3.3) Lab identification of specimens cross-referenced with the original identification

Type	Specimen Lab ID #	Pipe	Section	Degrees (from/to)	Type	Specimen Lab ID #	Pipe	Section	Degrees (from/to)
R	R1	A	2	0/90	Z	Z1	A	2	270/360
	R2	A	2	180/270		Z2	A	2	0/90
	R3	A	1	270/360		Z3	B	1	270/360
	R4	A	1	180/270		Z4	B	1	180/270
	R5	B	1	90/180		Z5	B	1	90/180
	R6	B	2	270/360		Z6	B	2	270/360
	R7	B	2	180/270		Z7	B	2	180/270
	R8	B	2	90/180		Z8	B	2	90/180
	R9	B	2	0/90		Z9	B	2	0/90
	R10	A	2	90/180		Z10	A	1	270/360
	R11	B	1	270/360		Z11	A	1	180/270
	R12	A	1	90/180		Z12	A	1	90/180
	R13	A	2	270/360		Z13	A	2	90/180
	R14	B	1	180/270		Z14	A	2	180/270
	RA	A	1	0/90		ZA	A	1	0/90
	RB	B	1	0/90		ZB	B	1	0/90

Figure (3.2) RC pipe specimens as received with FDOT identification

3.2.2 Characterization of RC Pipe Specimens

For all the as-cut specimens measurement of the interior concrete cover thickness was made by direct ruler readings on the four cut edges at all exposed reinforcing wires. Statistical analysis of data for pipe sections from each manufacturer indicated that Z-type specimens have a thicker internal cover (ranging from 0.6" to 1.75") than R-type specimens (ranging from 0.4 in to 1.1 in) as shown in Figure 3.3 and Table 3.4. In order to establish the variability in cover thickness over longitudinal versus circumferential (transverse) steel wires, measurements were also made on each two opposite edges of each specimen. Figures 3.4 to 3.7 show that circumferential reinforcing wires had a slightly larger concrete cover thickness than that of longitudinal reinforcing wires.

In the Z-type specimens conspicuous consolidation gaps were visible in most instances around circumferential reinforcing steel wires apparently due to unconsolidated concrete, Figures 3.8 & 3.9.The gaps were nearly always on the bell side of the circumferential steel wire which may be attributed to pipe construction related reasons. The gaps seemed to be forming a tunnel running along the entire length of wires. The existence of a continuous gap along the entire length of wire was clearly evident when the cracked specimens exhibited water leaks through the gaps on the four sides during a leak test.

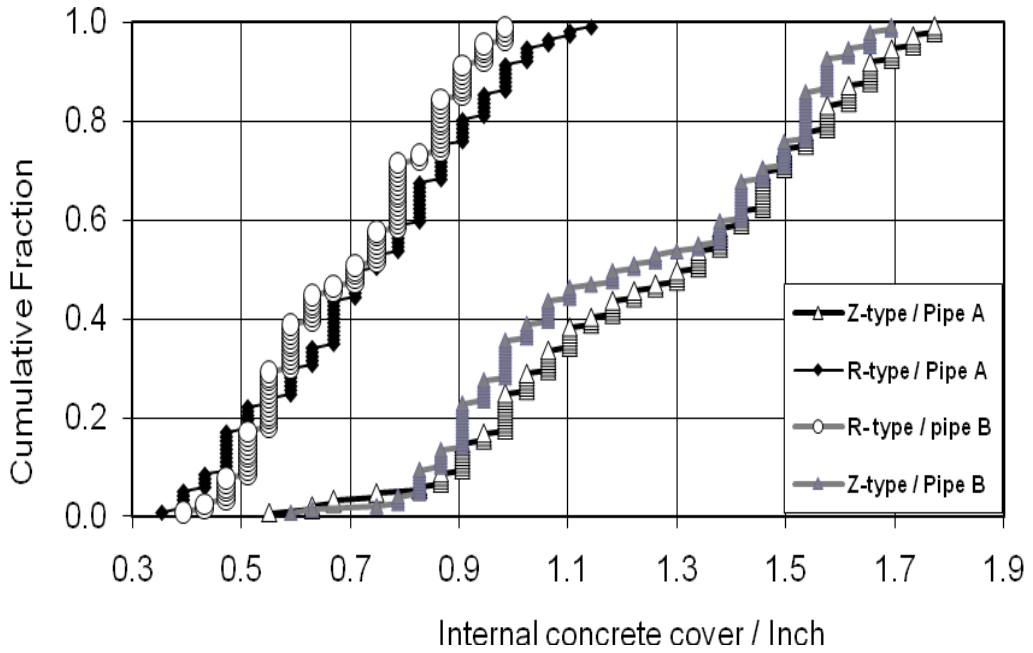

Figure (3.3) Interior concrete cover thickness for all specimens grouped by the pipes from which they were extracted (values measured on the four edges of a specimen)

Table (3.4) Interior concrete cover thickness for the R- and Z-type specimens (measured at exposed steel wires on the four edges of a specimen)

Specimen	Concrete Cover *l* in		Specimen	Concrete Cover *l* in	
	Average	*Stdev*		*Average*	*Stdev*
RA	0.498	0.115	*ZA*	1.258	0.361
RB	0.503	0.060	*ZB*	1.253	0.277
R1	0.627	0.115	*Z1*	1.308	0.285
R2	0.861	0.120	*Z2*	1.323	0.251
R3	0.734	0.104	*Z3*	1.339	0.232
R4	0.936	0.100	*Z4*	1.093	0.299
R5	0.686	0.118	*Z5*	1.144	0.345
R6	0.796	0.145	*Z6*	1.282	0.251
R7	0.846	0.106	*Z7*	1.144	0.220
R8	0.655	0.112	*Z8*	1.249	0.329
R9	0.560	0.054	*Z9*	1.249	0.340
R10	0.675	0.223	*Z10*	1.376	0.353
R11	0.687	0.164	*Z11*	1.045	0.331
R12	0.741	0.273	*Z12*	1.384	0.189
R13	0.748	0.083	*Z13*	1.315	0.229
R14	0.834	0.083	*Z14*	1.126	0.251

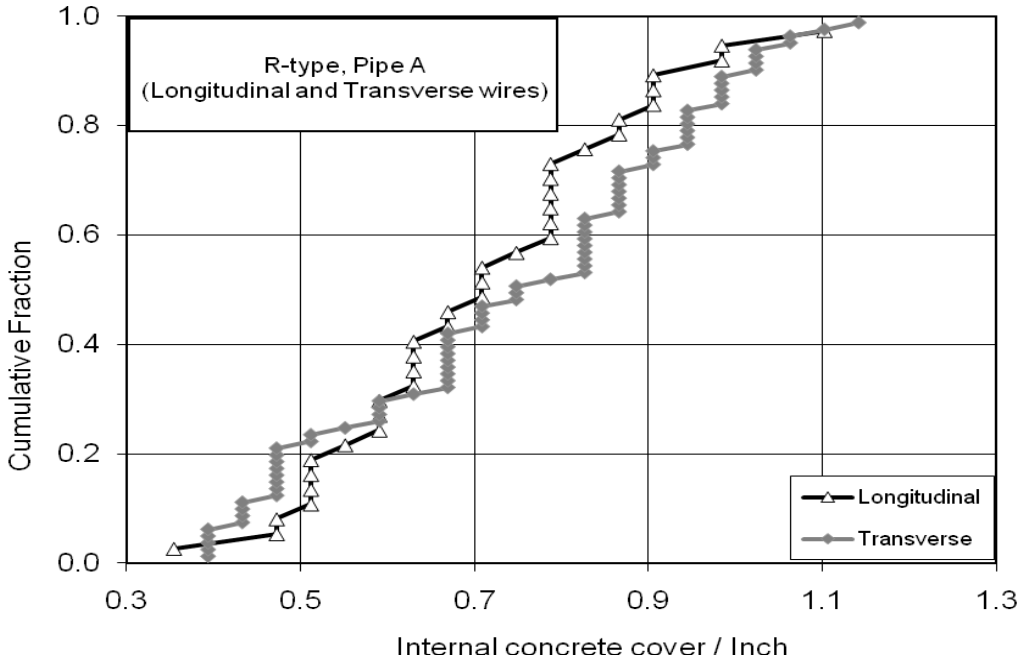

Figure (3.4) Interior concrete cover thickness on longitudinal and transverse wires for R-type, pipe A (values measured on two respective opposite edges of a specimen)

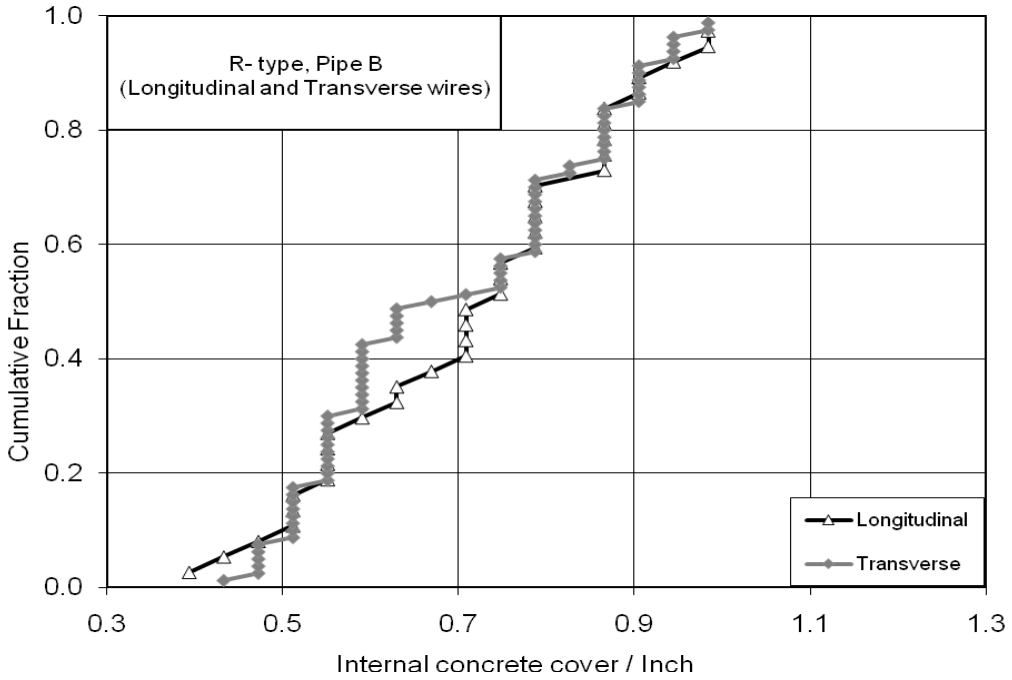

Figure (3.5) Interior concrete cover thickness on longitudinal and transverse wires for R-type, pipe B (values measured on two respective opposite edges of a specimen)

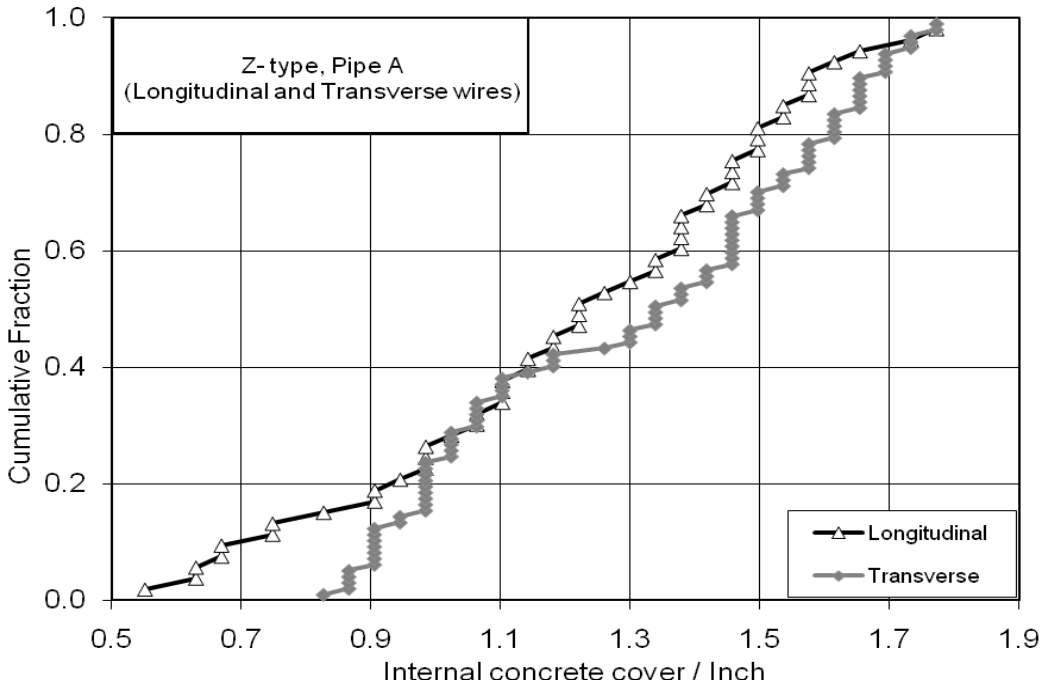

Figure (3.6) Interior concrete cover thickness on longitudinal and transverse wires for Z-type, pipe A (values measured on two respective opposite edges of a specimen)

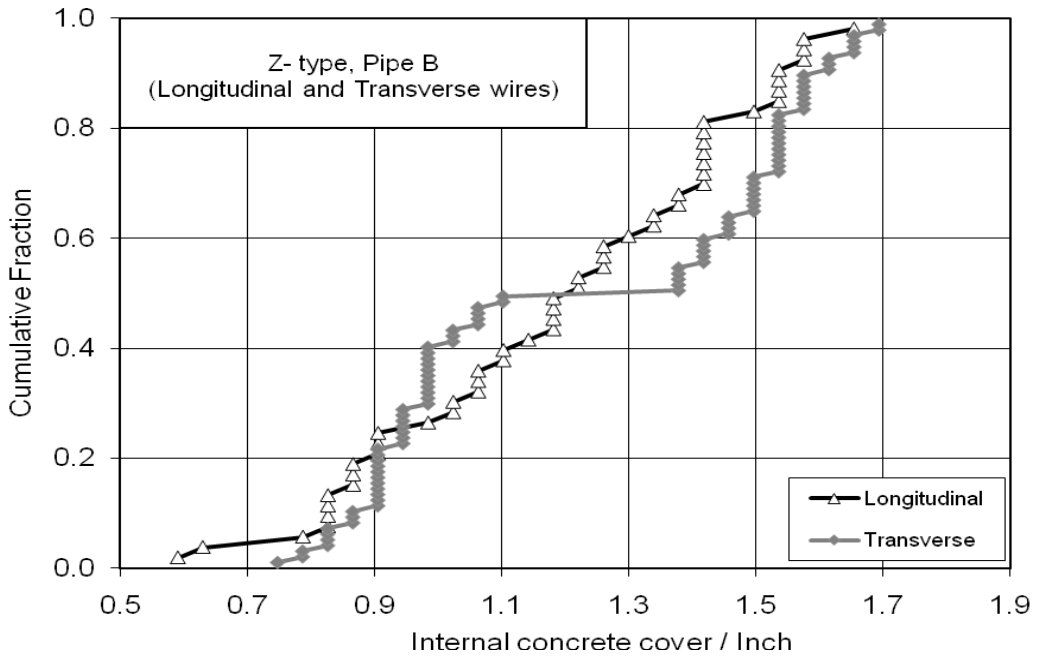

Figure (3.7) Interior concrete cover thickness on longitudinal and transverse wires for Z-type, pipe B (values measured on two respective opposite edges of a specimen)

Figures 3.10 and 3.11 show the interior concrete cover thickness measurements for the individual specimens intended for the corrosion exposure experiment. Using an ohmmeter, all wires exposed at the edges of each specimen used in the corrosion tests were found to be mutually electrically continuous.

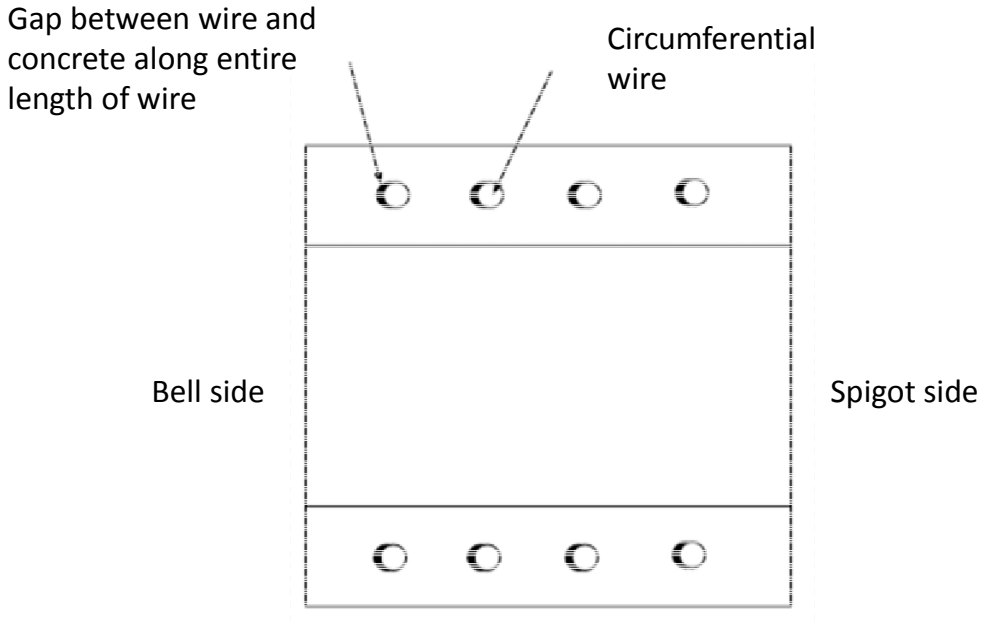

Figure (3.8) a schematic showing the top view of a Z-type specimen illustrating voids observed around circumferential wires

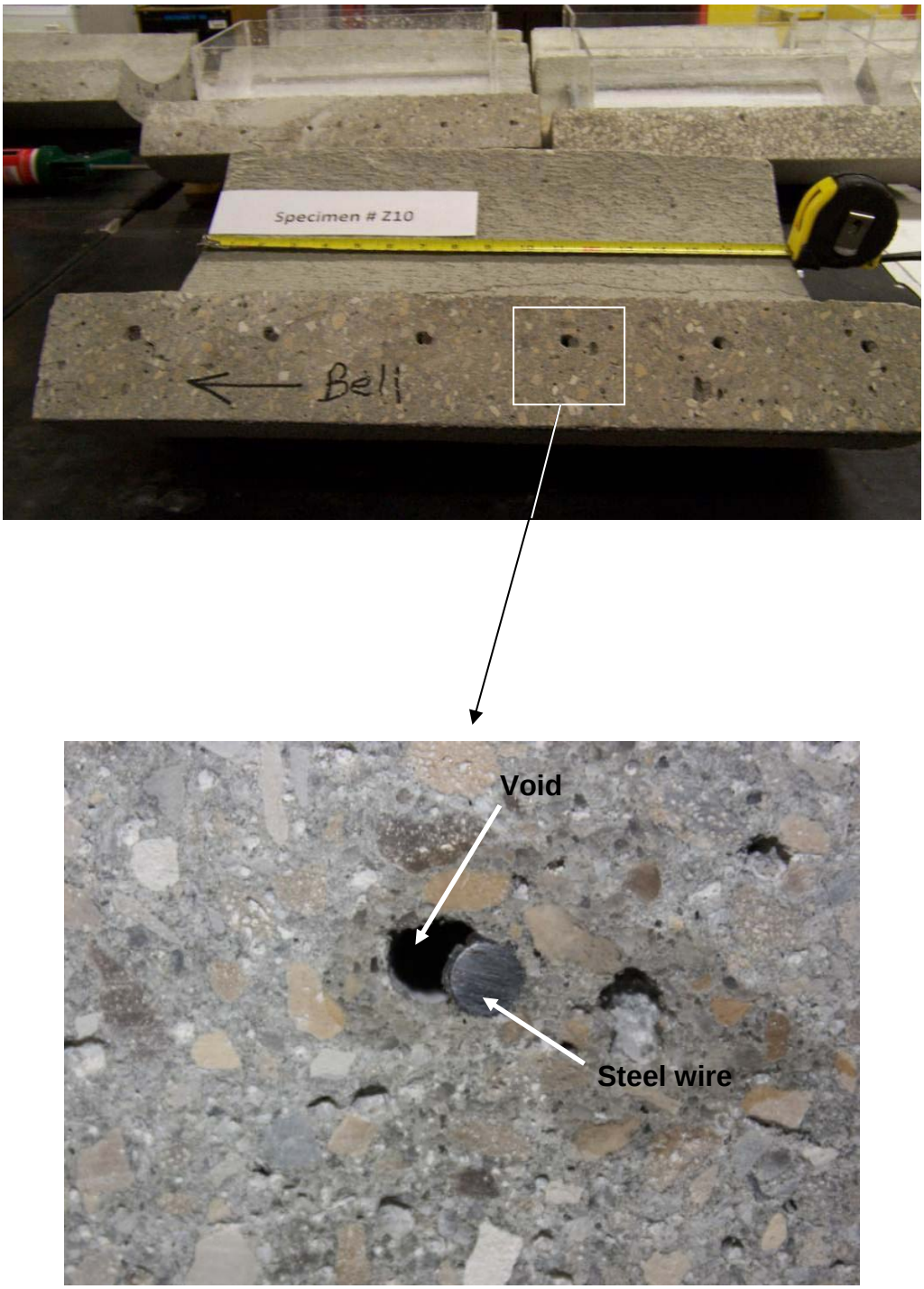

Figure (3.9) an example of a Z-type specimen showing consolidation voids next to circumferential wires with a magnified image showing the wire/void details

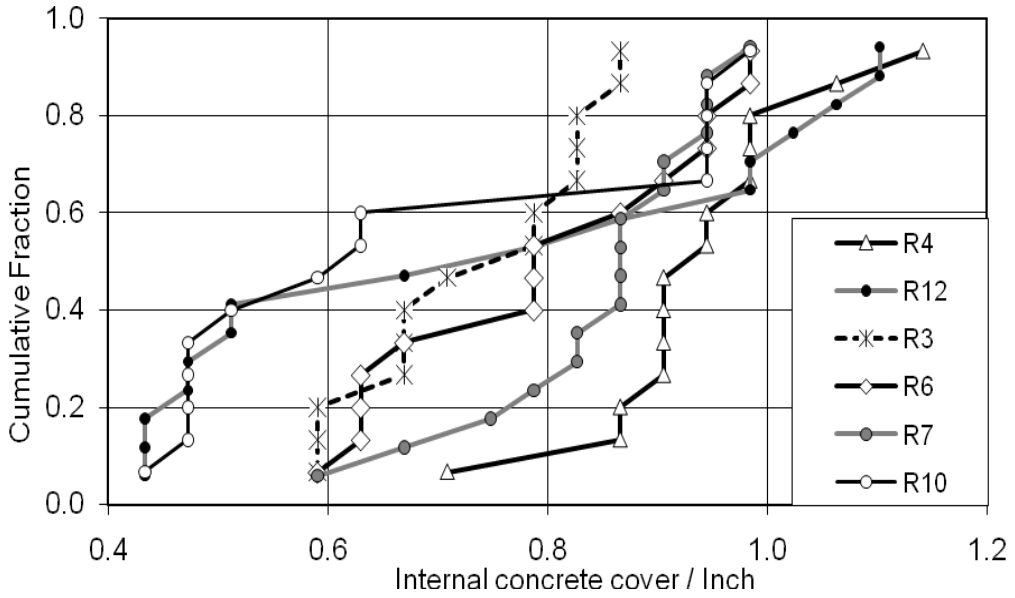

Figure (3.10) Interior concrete cover thickness for individual R-type quadrants to be used in the corrosion exposure experiment (values measured on the four edges of a specimen)

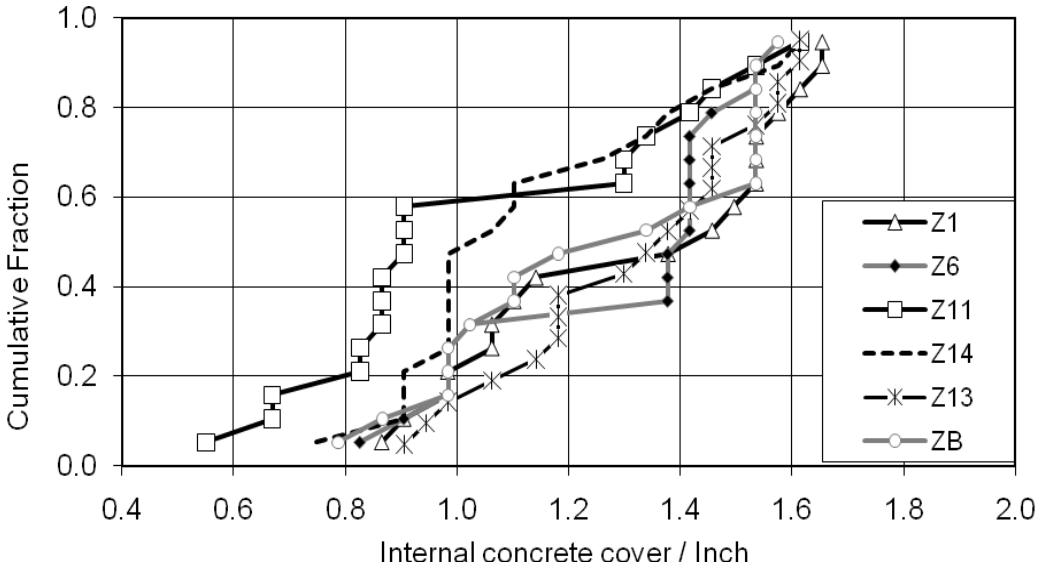

Figure (3.11) Interior concrete cover thickness for individual Z-type quadrants to be used in the corrosion exposure experiment (values measured on the four edges of a specimen)

3.2.3 Generation of Interior Surface Cracks

The cracks were intended to be single, extending lengthwise from the bell side to the spigot side of a specimen for a total length of 18 in. Figure 3.12 shows the cracking rig, operated with an MTS 810 (model # 204.91) testing frame using three-point loading.

Figure (3.12) Cracking rig used to generate cracks in RC culvert pipe specimens

The crack width was controlled with a measuring gauge comprised of two nuts bonded to the surface of concrete on either the bell or spigot end, on both sides of the area in which a crack was to be induced. The distance between the nut edges was measured using a digital caliper before and during cracking as shown in Figure 3.13. Trial tests established the amount of loaded deviation between the nut edges needed to achieve the desired crack width upon release of the load. The cracks were, as intended, generally single and quite uniform as exemplified in Figures 3.14 a & b. Force application was increased by manual control with the procedure completed in about 5 minutes. The amount of force required to achieve a final relaxed crack opening of 0.02 in was about 6000 to 8000 lb. For the 0.1-in-openings the force was about 8000 to 10000 lb for both the Z-Type and R-Type specimens.

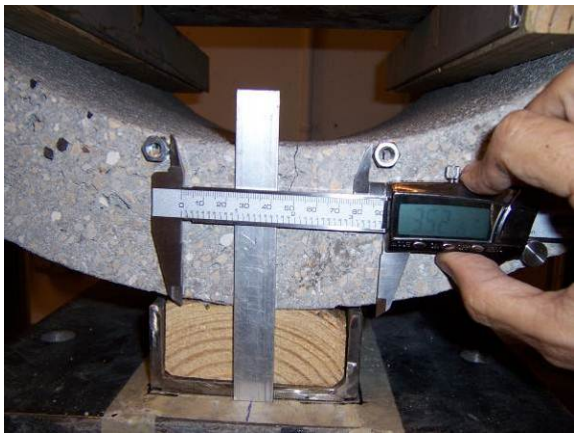

Figure (3.13) Crack width measuring procedure

After cracking was completed, more detailed measurements of crack width were performed using a CTL crack comparator at ½ in intervals along the entire length of a crack. An approximate measurement to establish the apparent crack depth was also conducted using an insertion gauge. The insertion gauge was a 0.3 mm diameter wire in the case of specimens having a crack width of 0.02 in. In the case of specimens having a crack width of 0.100 in a thin gage of dimensions ~ 4 mm x 0.75 mm was used.

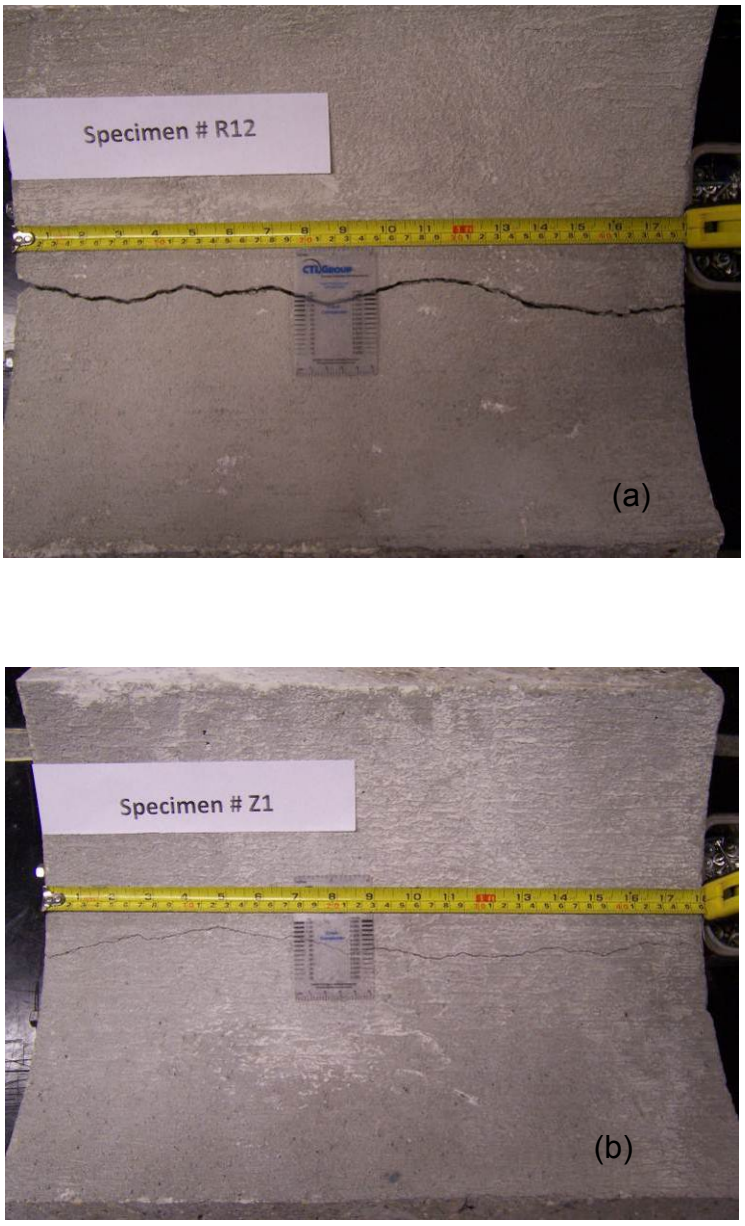

Figure (3.14) Crack width measurement using a crack comparator along the entire crack length at 0.5 in intervals for (a) 0.100 in-R-type specimen and (b) 0.020 in-Z-type specimen

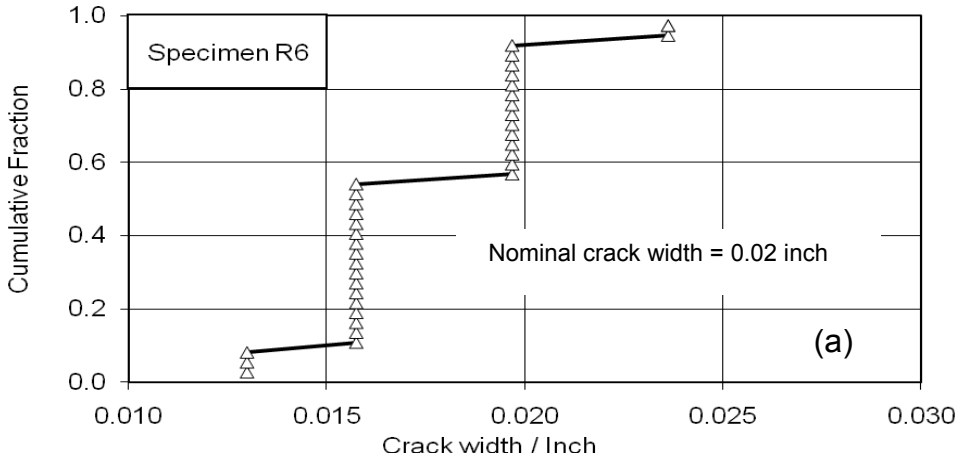
Specimen R6
Nominal crack width = 0.02 inch
(a)
Cumulative Fraction
Crack width / Inch
1.0
0.8
0.6
0.4
0.2
0.0
0.010
0.015
0.020
0.025
0.030

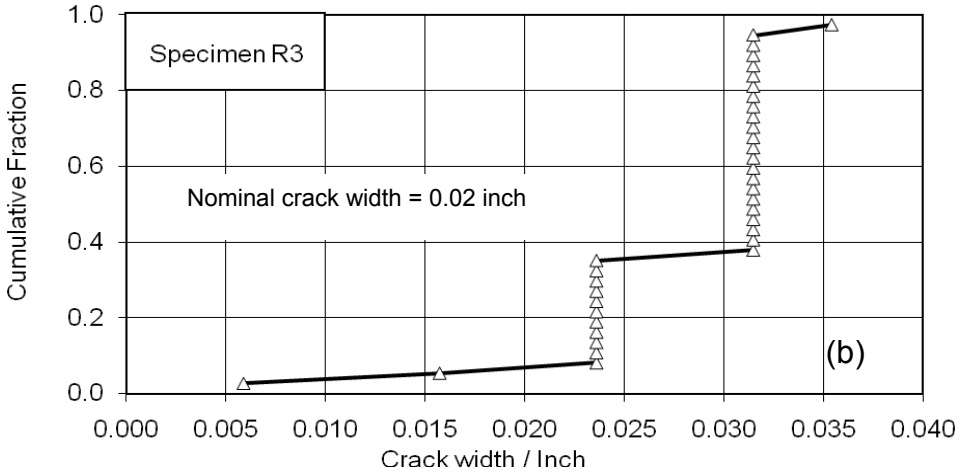
Specimen R3
Nominal crack width = 0.02 inch
(b)
Cumulative Fraction
Crack width / Inch
1.0
0.8
0.6
0.4
0.2
0.0
0.000
0.005
0.010
0.015
0.020
0.025
0.030
0.035
0.040

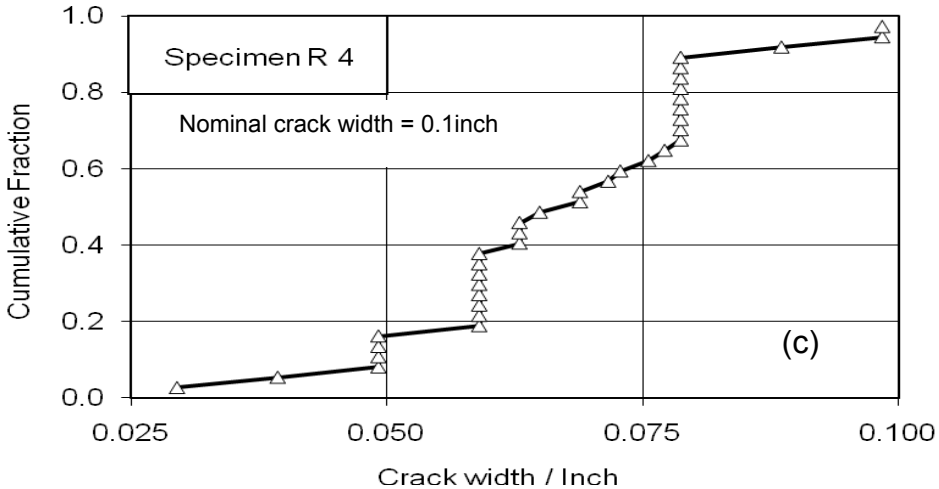
Specimen R 4
Nominal crack width = 0.1inch
(c)
Cumulative Fraction
Crack width / Inch
1.0
0.8
0.6
0.4
0.2
0.0
0.025
0.050
0.075
0.100

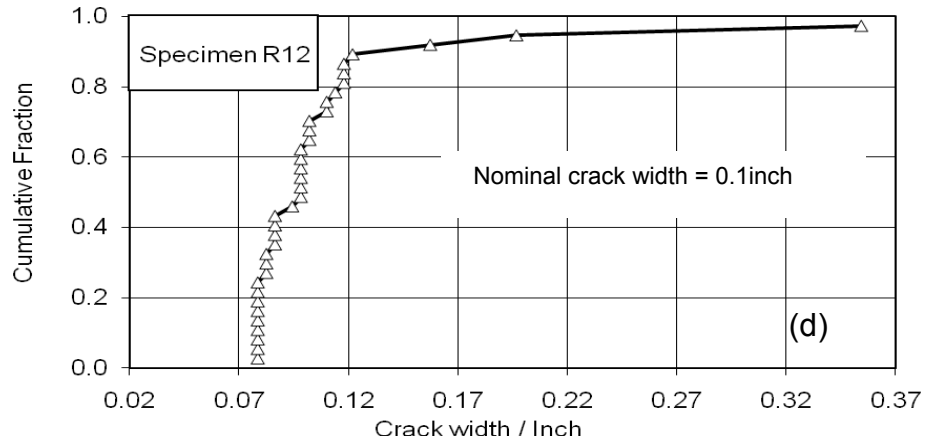
Specimen R12
Nominal crack width = 0.1inch
(d)
Cumulative Fraction
Crack width / Inch
1.0
0.8
0.6
0.4
0.2
0.0
0.02
0.07
0.12
0.17
0.22
0.27
0.32
0.37

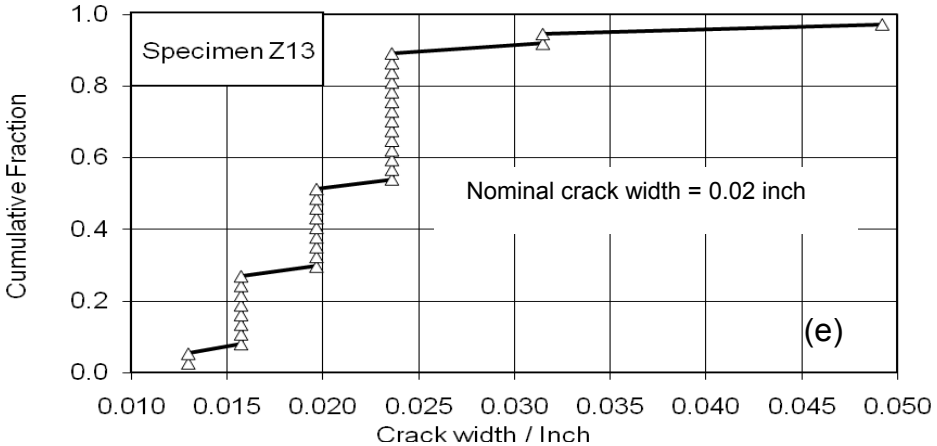
Specimen Z13
Nominal crack width = 0.02 inch
(e)
Cumulative Fraction
Crack width / Inch
1.0
0.8
0.6
0.4
0.2
0.0
0.010
0.015
0.020
0.025
0.030
0.035
0.040
0.045
0.050

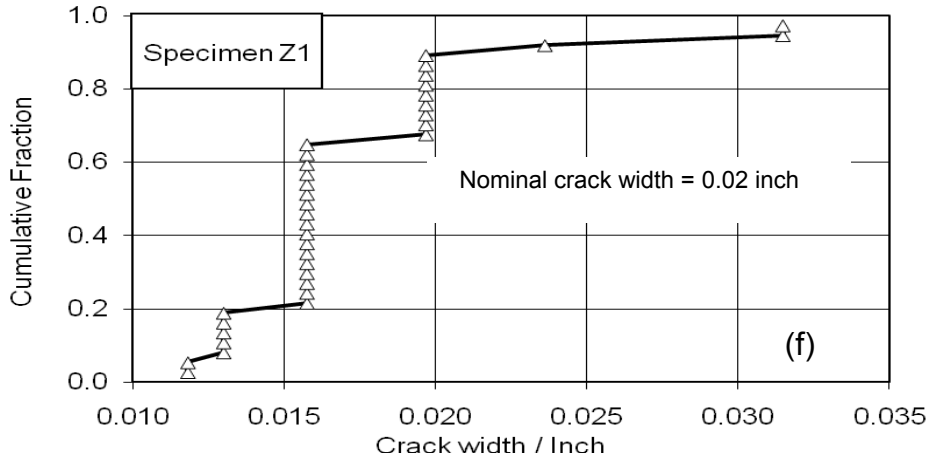
Specimen Z1
Nominal crack width = 0.02 inch
(f)
Cumulative Fraction
Crack width / Inch
1.0
0.8
0.6
0.4
0.2
0.0
0.010
0.015
0.020
0.025
0.030
0.035

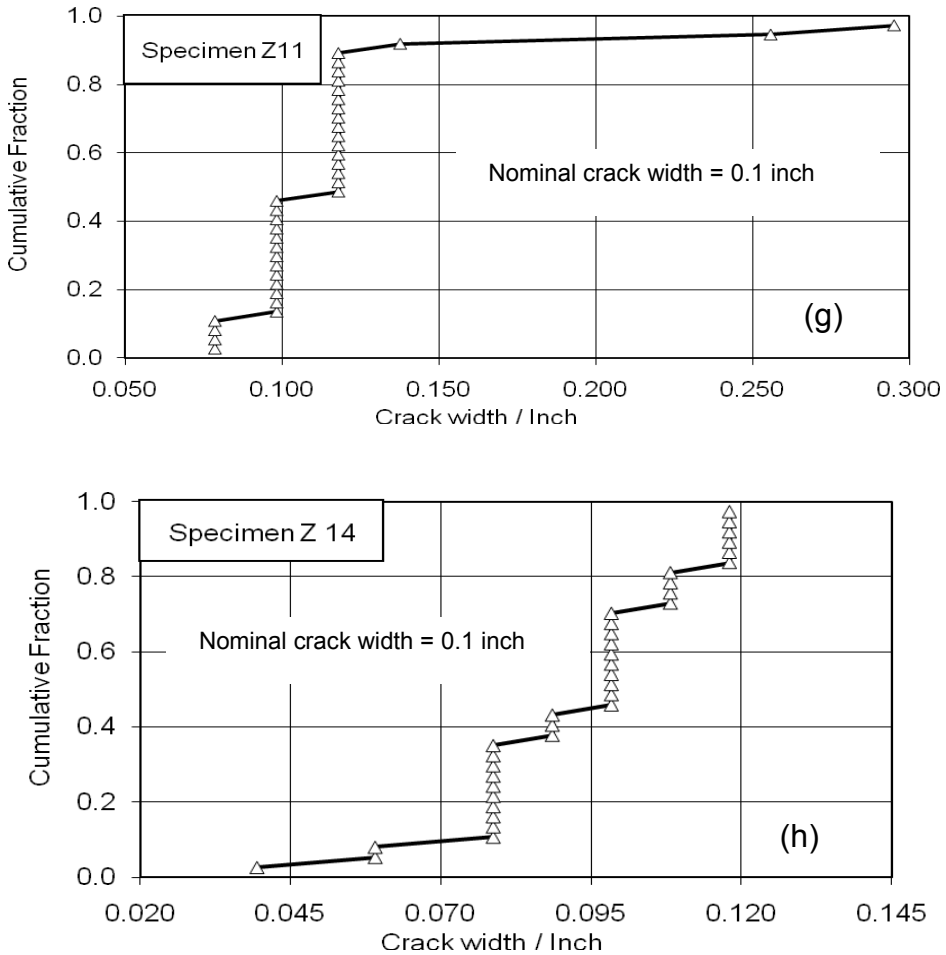

Figure (3.15) Crack width measurements using a crack comparator for each individual cracked quadrant intended for the corrosion exposure experiment, R-type (a) to (d) and Z-type (e) to (h)

Table 3.5 shows the achieved crack width and depth values for all cracked specimens. The table also shows whether the cracks were apparently intersecting the reinforcing steel wire. That was nominally established by comparing the maximum and average crack depth measured across the entire length of a crack with the average depth of reinforcing steel for that particular specimen. In general the depth of the 0.100-in-width cracks, as determined by the procedure indicated earlier, was greater than that for the 0.02-in-width cracks.

Table (3.5) Crack width and depth data for R- and Z-type specimens

Type	Specimen #	Target crack width / in	Average internal cover / in	Achieved crack Width / in		Average achieved crack depth* / in	Average crack depth intersecting wire	Maximum crack depth intersecting wire	Remark
				Average	Standard deviation				
R	R7	0	0.846	-	-	-	-	-	Control
	R10		0.675	-	-	-	-	-	Control
	R3	0.02	0.734	0.028	0.006	0.331			
	R6		0.796	0.018	0.003	0.254			
	R1		0.627	0.027	0.019	0.284			
	R5		0.686	0.019	0.006	0.192			
	R14		0.834	0.023	0.006	0.373		Yes	
	R2		0.861	0.025	0.005	0.327			
	R12	0.100	0.741	0.106	0.049	1.288	Yes	Yes	
	R4		0.936	0.067	0.015	1.124	Yes	Yes	
	R9		0.56	0.088	0.026	1.07	Yes	Yes	
	R11		0.687	0.074	0.027	0.852	Yes	Yes	
	R13		0.748	0.0778	0.015	0.906	Yes	Yes	
	RB		0.503	0.083	0.036	0.984	Yes	Yes	
Z	Z6	0	1.282	-	-	-	-	-	Control
	ZB		1.253	-	-	-	-	-	Control
	Z1	0.020	1.308	0.017	0.004	0.196			
	Z13		1.315	0.021	0.006	0.208			
	Z7		1.144	0.024	0.003	0.272			
	Z5		1.144	0.02	0.003	0.232			
	Z4		1.093	0.021	0.003	0.244			
	Z3		1.339	0.021	0.005	0.306			
	Z11	0.100	1.045	0.116	0.042	1.343	Yes	Yes	
	Z12		1.384	0.111	0.028	1.331		Yes	
	Z9		1.249	0.07	0.013	0.992		Yes	
	Z8		1.249	0.113	0.012	1.48	Yes	Yes	
	Z14		1.126	0.093	0.019	1.18	Yes	Yes	
	Z10		1.376	0.094	0.030	1.02		Yes	

* Depth measured with a 0.3 mm diameter wire for specimens having crack width ~ 0.020 in and by inserting a thin gage of dimension (4 mm x 0.75 mm) for specimens having crack width ~ 0.100 in. Each specimen had 36 data points for crack depth and 36 data points for crack width.

3.3 Pond Preparation

Plexiglas exposure ponds were fabricated and attached to the cracked specimens and uncracked control specimens. The pond footprint area was 9 in x 14 in. The four sides of the ponds were sealed with silicone sealant to prevent leaks. Both crack ends as well as the area at the back side of the specimen facing the crack were also sealed with epoxy to prevent leak through the crack, as exemplified in Figure 3.16. Likewise, any gaps or voids around steel wires were sealed with silicone sealant. The ponds contained 2 liters of solution, which was enough to cover the entire footprint zone with an extra ¼ in of liquid at the edges.

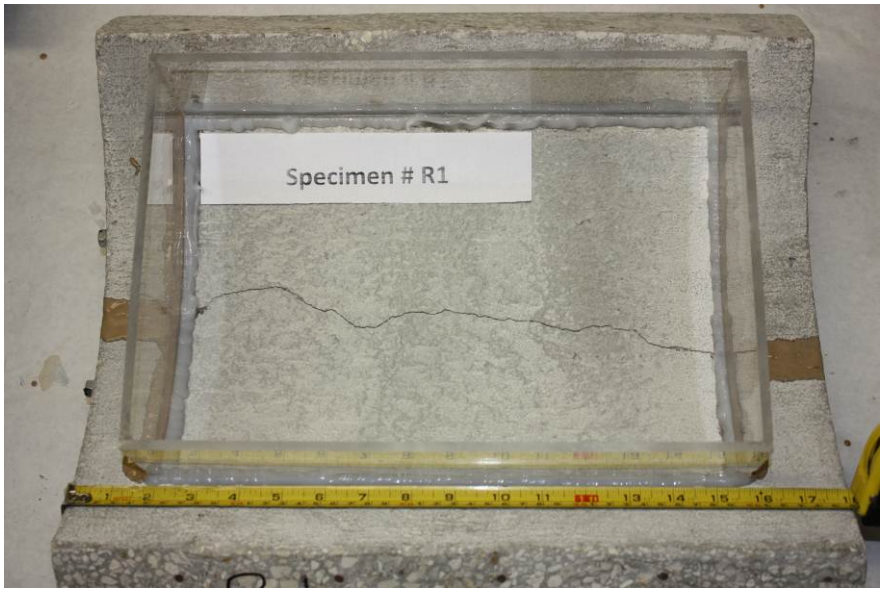

Figure (3.16) A specimen with a Plexiglas exposure pond attached and crack ends sealed with epoxy

3.3.1 Autogenous Healing Tests

A total of 16 cracked specimens in table 3.6, of both the Z- and R-type, having crack widths of 0.020 in and 0.100 in, were exposed to a saturated calcium hydroxide solution, (2.5 g of $Ca(OH)_2$ salt in 1 liter of distilled water), $Ca(OH)_2$, under 48-hour wet / 48-hour dry cycling for a period of two months in lab temperature conditions (~ 25^{o}C). Fresh calcium hydroxide solution was used for each specimen at every wet cycle to compensate for wastage due to carbonation from atmospheric CO_2 during the previous cycle. In the dry cycle, the specimen was drained using a water vacuum pump. The cracks were examined using a portable microscope regularly during the test period to check for any substantial healing product formation or crack closure. Figure 3.17 shows a specimen during a wet cycle.

Table (3.6) Specimens exposed to autogenous healing environment

Crack width	0.020 in	0.100 in
Specimen #	Z3	Z8
	Z4	Z9
	Z5	Z10
	Z7	Z12
	R1	R9
	R2	R11
	R5	R13
	R14	RB

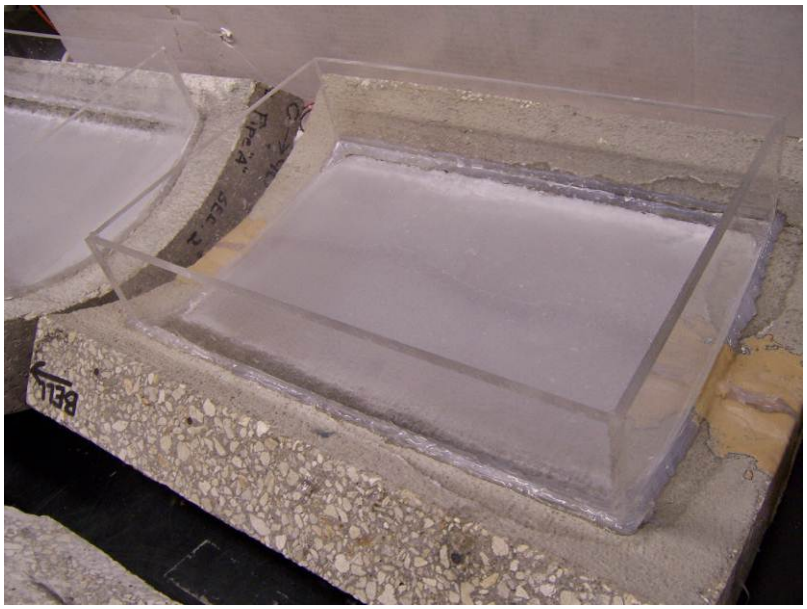

Figure (3.17) A cracked specimen during exposure to healing solution

3.3.2 Corrosion Experiment

The cracked and uncracked specimens from both the R- and Z-type specimens shown in Table 3.7, were tested for corrosion resistance. As indicated earlier, these tests were conducted only for the untreated crack condition. All exposures were conducted at lab temperature of ~ 25^{o}C. The corrosion specimens were first subjected to continuous ponding with de-ionized (DI) water for 33 days (Figure 3.18). This prior exposure to DI water was conducted to allow the specimen steel potentials to reach a steady state condition in a low aggressiveness environment, thus allowing for further insight on the effect of introducing the more aggressive medium for the main portion of the test. After 33 days the ponding medium was changed to distilled water with the addition of sodium chloride to obtain

a 500 ppm chloride ion concentration. Results reported here correspond to the period of 2 to 3 months following that change. The solution as prepared was near neutral but pH in the pond stabilized to a value of ~ 8.7 at the end of that one-month period. Figure 3.18 shows a cracked specimen during exposure to the chloride solution. In order to establish a baseline and a trend in potential change, the reinforcing steel potentials were measured regularly before and during exposure to chloride. All potential measurements were made using a saturated calomel reference electrode (SCE) placed at the center of the pond with its tip immersed in water. Electrochemical Impedance Spectroscopy (EIS) testing was performed to determine the corrosion current of embedded reinforcing steel before and after exposure to the chloride containing solution. The EIS test was conducted using Solartron impedance equipment (Potentiostat and Analyzer SI 1287 & SI 1260). The frequency range evaluated had an upper end of 1000 Hz. The lower end was 10 mHz (during the chloride-free exposure period) or 3 mHz (after chloride addition) for additional fast measurements that could be conducted easily, and 1 mHz or 0.2 mHz for slower experiments designed to better sample the lower frequency range which typically contains much of the information relevant to corrosion rate determination. Excitation amplitude was 10 mV. The reference electrode used was the SCE placed in the solution same as in the potential measurements. The counter electrode was an activated titanium mesh immersed in solution and covering the entire pond footprint.

Table (3.7) Specimens evaluated in the corrosion experiment

Crack width	Uncracked (Control)	0.020"	0.100"
Specimen #	Z6	Z1	Z11
	ZB	Z13	Z14
	R7	R3	R4
	R10	R6	R12

The equivalent circuit shown in Figure 3.19 was used for simplified interpretation of the electrochemical impedance data (see Sagüés (1993) for background information), and consists of a solution resistance Rs connected in series with a parallel combination of a polarization resistance component Rp, associated with the corrosion process, with a constant phase angle element CPE component representing an interfacial charge storage process. The CPE has impedance Z_{CPE} given by:

$$Z_{CPE} = 1/ [Y_o (j \omega)^n] \qquad \text{Eq. (3.1)}$$

Where; Y_o is a constant and n is a real number between 0 and 1; $j = (-1)^{1/2}$ and $\omega = 2 \pi f$ (where f is frequency).

The equivalent circuit total impedance Z_T is given by:

$$Z_T = R_s + \{ 1 / [Y_o (j \omega)^n + R_p^{-1}] \} \qquad \text{Eq. (3.2)}$$

For the tests conducted to lowest frequencies of 0.2 mHz or 1 mHz the impedance parameters Rs, R_p, Y_o and n were determined by fitting the measured total impedance data over a selected frequency range with the equivalent circuit total impedance values over the same range. The selected frequency range consisted of the data for the lowest frequency decade sampled during the test.

The corrosion current (I_{corr}) was estimated by:

$$I_{corr} = B / Rp \qquad \text{Eq. (3.3)}$$

Where B is Stern-Geary coefficient and is approximated as 26 mV for corroding steel in concrete (Andrade, 1978; Sagüés 1993).

Figure (3.18) A cracked specimen during exposure to the chloride solution

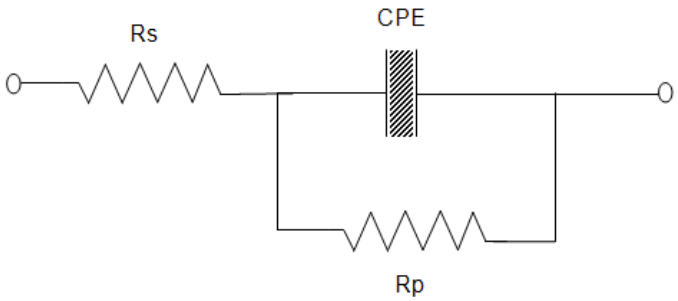

Figure (3.19) Equivalent circuit used for interpreting EIS data

When the lowest frequency in the measured EIS spectrum was higher than 1 mHz, the parameters obtained with the above procedure were found to be affected by large uncertainty. An alternative procedure using a rough correction approach was employed in those cases, estimating polarization resistance and corrosion current for each specimen as follows:

a) A provisional value of polarization resistance Rpp, based on the datum for the lowest frequency in the EIS spectrum, was obtained by:

$$Rpp = [(Z' - Rs)^2 + Z''^2]^{1/2} \qquad \text{Eq. (3.4)}$$

Where; Z' and Z" are the real and imaginary parts respectively of the impedance at the lowest frequency, as illustrated in Figure 3.20.

Rpp is smaller than the actual value of the polarization resistance Rp, which would have required tests conducted to lower frequencies to be evaluated with less uncertainty. On first approximation, it was assumed that for a given lowest frequency f_L used to obtain Rpp there is direct proportionality between Rpp and Rp. It was further assumed that for each specimen the corresponding proportionality factor $PF(f_L)$ remains unchanged with time, so it could be determined using the data from one of the tests conducted using a low frequency limit of 1mHz or less. That procedure is illustrated in the next two steps.

b) As an example, consider the case of an EIS test of a given specimen where f_L=10 mHz. Analyze the EIS data from the same specimen for another test when the lowest frequency was 1 mHz, and note the value Rp obtained then. Consider the 10 mHz datum for that test and treat it as if it were the lowest frequency per the procedure in (a). Call Rppe the resulting value. Estimate PF by the following:

$$PF = Rp / Rppe \qquad \text{Eq. (3.5)}$$

c) Apply to proportionality factor PF to the Rpp value calculated per (a) in the test with f_L= 10 mHz and obtain a corrected value of polarization resistance Rpc as follows:

$$Rpc = Rppe \; PF \qquad \text{Eq. (3.6)}$$

Figure 3.21 shows an example of the application of this procedure. The Rpp values strongly underestimate Rp, but upon correction the Rpc values better approximate the trend obtained from EIS tests performed with the lowest test frequency limits.

The value of I corr was then calculated using Eq. (3.3) but using Rpc instead.

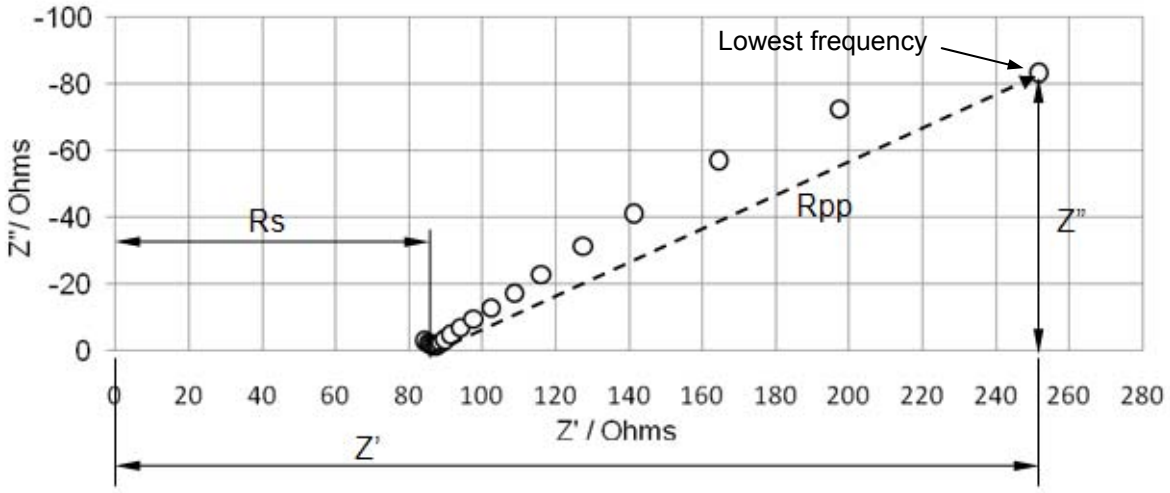

Figure (3.20) Estimation of provisional Rp value (Rpp) for EIS measurements with a lowest frequency higher than 1 mHz. Measured EIS data are indicated on the graph by circles and the estimated Rpp value is indicated by the length of a broken line

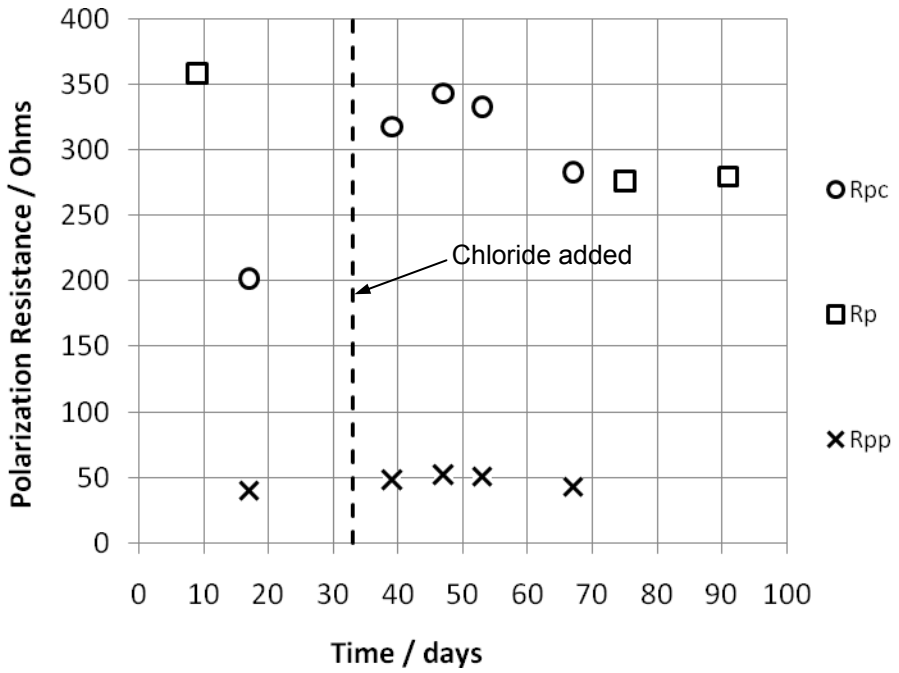

Figure (3.21) An example with specimen # Z14, showing the provisional and corrected values of polarization resistance (Rpp & Rpc respectively) for EIS measurements having lowest frequency higher than 1 mHz and Rp values for EIS measurements having lowest frequencies of 1 mHz and 0.2 mHz

4 RESULTS AND DISCUSSION

4.1 Autogenous Healing

Upon exposure for 2 months, visual examination of the specimens, subjected to wet / dry cycling of saturated calcium hydroxide solution, revealed that no clear sings of healing of the cracks (Figures 4.1 to 4.4). There was no change in crack size detected when the crack width and depth were measured.

Figure (4.1) Z-type specimen with 0.100-in-wide crack after exposure to saturated calcium hydroxide solution

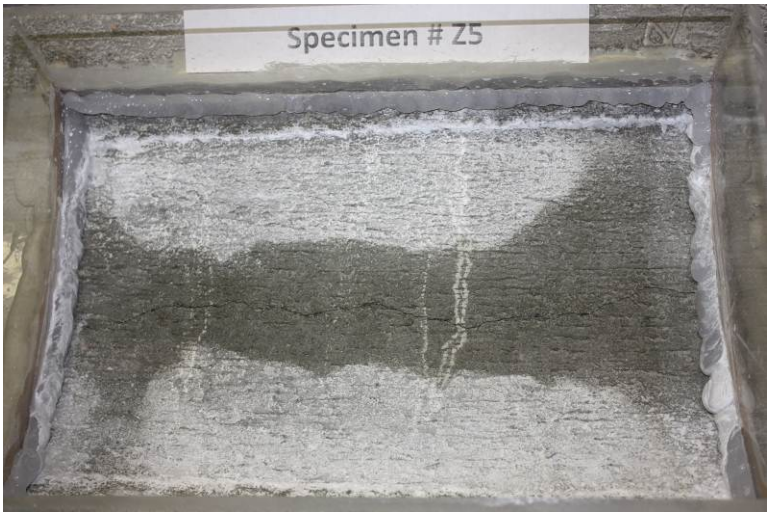

Figure (4.2) Z-type specimen with 0.02-in-wide crack after exposure to saturated calcium hydroxide solution

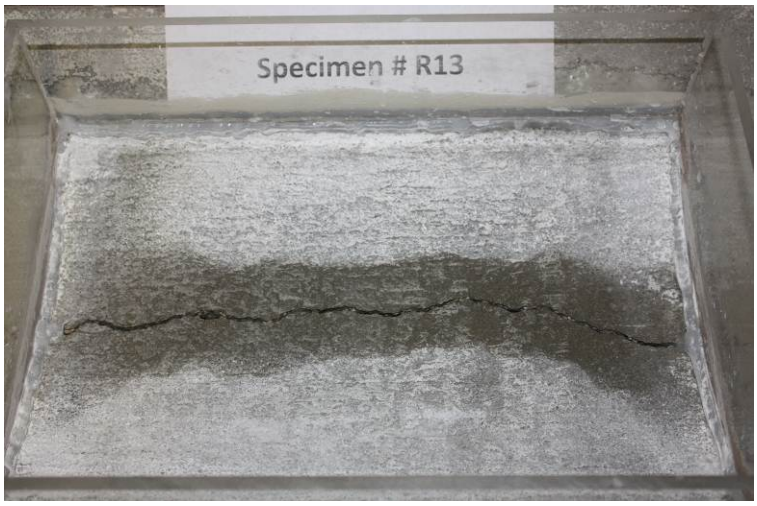

Figure (4.3) R-type specimen with 0.100-in-wide crack after exposure to saturated calcium hydroxide solution

Figure (4.4) R-type specimen with 0.02-in-wide crack after exposure to saturated calcium hydroxide solution

Some of the specimens with 0.020-in-wide cracks exhibited an apparent precipitation within the crack, Figure 4.5. However, detailed examination showed that the product formed could easily be removed by a water jet leading to crack opening. That observation of apparent closure may, at best, be looked at as an initial stage of autogenous healing process. It was not possible to examine that finding in the limited project time frame. This finding is in agreement with Wagner's finding that an autogenous healing process can take up to several years to heal a crack of comparable crack widths (Neville 2002). In a similar study (Yang, 2009) of the healing process of cracked engineered cementitious material, it was found that the

maximum crack width which exhibited any healing was 150 μm (~ 0.006 in) after exposure to water for about 10 wet/dry cycles.

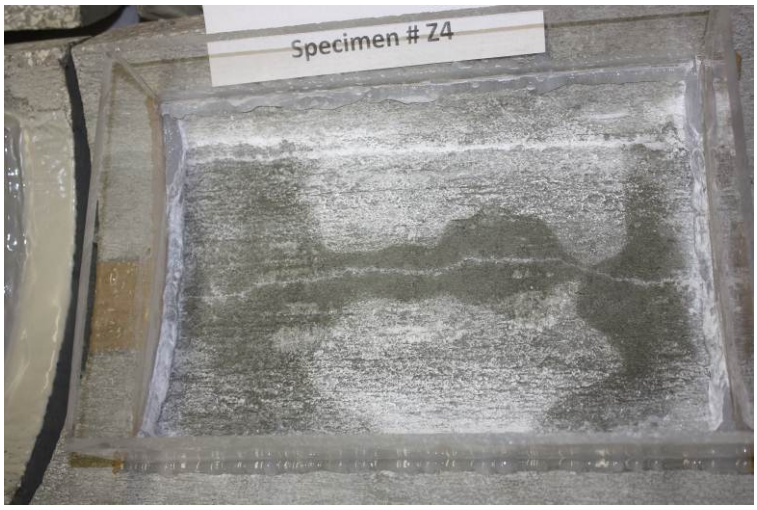

Figure (4.5) Z-type specimen with 0.02-in-wide crack showing apparent precipitation within the crack

4.2 Corrosion Experiment

4.2.1 Direct Observations

Some of the Z- and R-type specimens having 0.100-in-wide cracks (Z11 and R12) exhibited external visual signs of rust, Figures 4.6 to 4.9, as early as about one week after chloride exposure began. The specimens were exposed to DI water for 33 days before exposure to chloride). In each specimen, when first observed the corrosion product, was at one of the intersections of the circumferential steel wires with the crack.

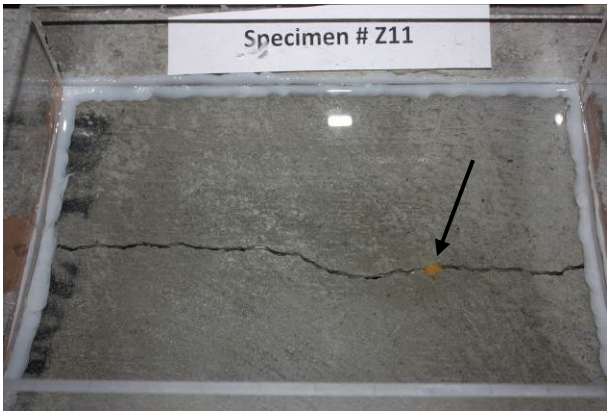

Figure (4.6) Specimen Z11 with 0.100-in-wide crack showing a corrosion spot at an intersection of the steel wire with the crack (indicated by the arrow) (6 days after the ponding solution started to incorporate chloride ion)

After 47 days of exposure to the chloride containing solution, new corrosion product was observed within the crack at specimen R4, Figure 4.11. The new corrosion product was not obvious and was discovered only when using a flash light for detailed crack inspection. There was no corrosion product observed in specimen Z14, Figure 4.12. The previously observed corrosion products in Z11 and R12 continued to grow as shown in Figures 4.7 and 4.9. More crack / wire intersections exhibited corrosion product build-up at specimen R12, Figure 4.10 while in specimen Z11 no new intersections exhibited any visible corrosion products. The greater concrete cover thickness in the case of the Z-type specimens may have caused the corrosion products to be less apparent at the crack mouth than in the case of R-type specimens. The corrosion product may also be filling the space provided by the consolidation gaps (typically found in the Z-type) around steel wires before transporting toward the crack mouth, thus resulting in less external manifestation of corrosion.

There was no sign of any corrosion product observed in any of the R- or Z-type specimens having 0.020-in-wide cracks, Figures (4.13 and 4.14).

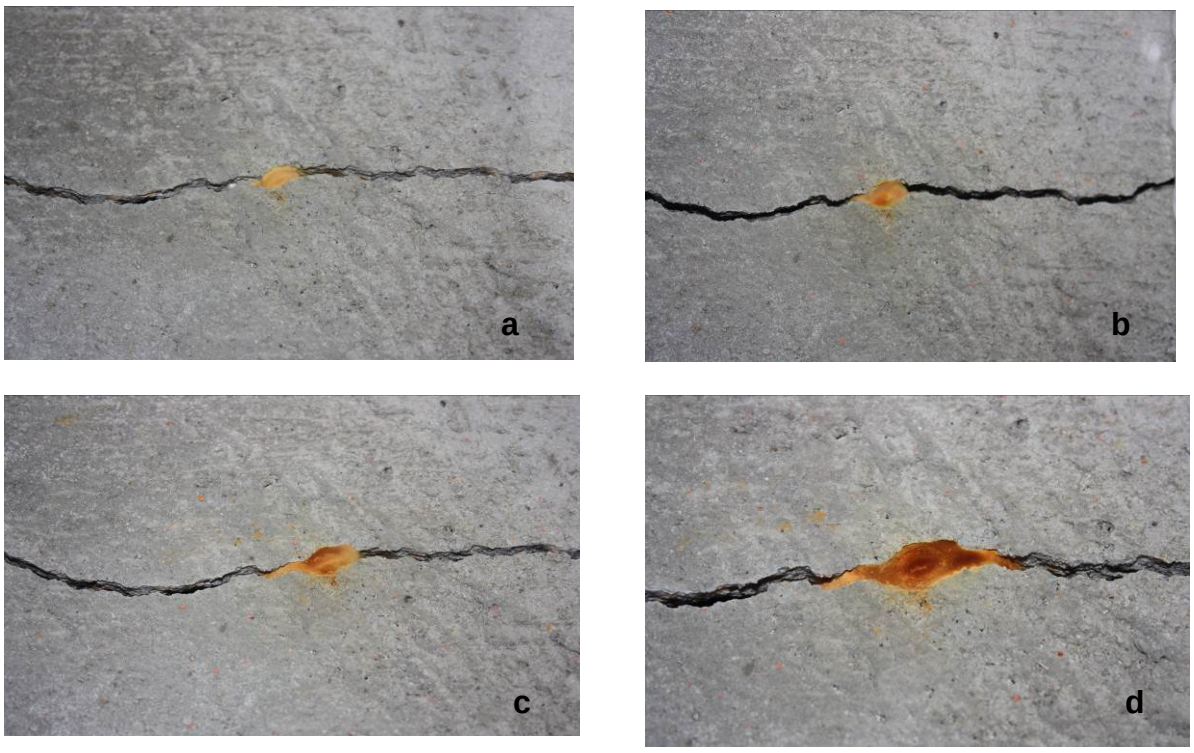

Figure (4.7) Corrosion product evolution in specimen Z11 (0.100-in-wide crack class) during exposure up to (a) 6 days (b) 20 days (c) 34 days (d) 52 days after the ponding solution started to incorporate chloride ion

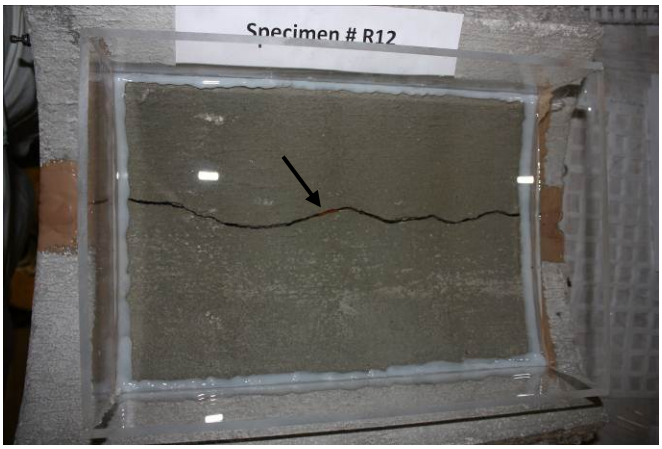

Figure (4.8) Specimen R12 with 0.100-in-wide crack showing a corrosion spot at an intersection of the steel wire with the crack (indicated by the arrow) (14 days after the ponding solution started to incorporate chloride ion)

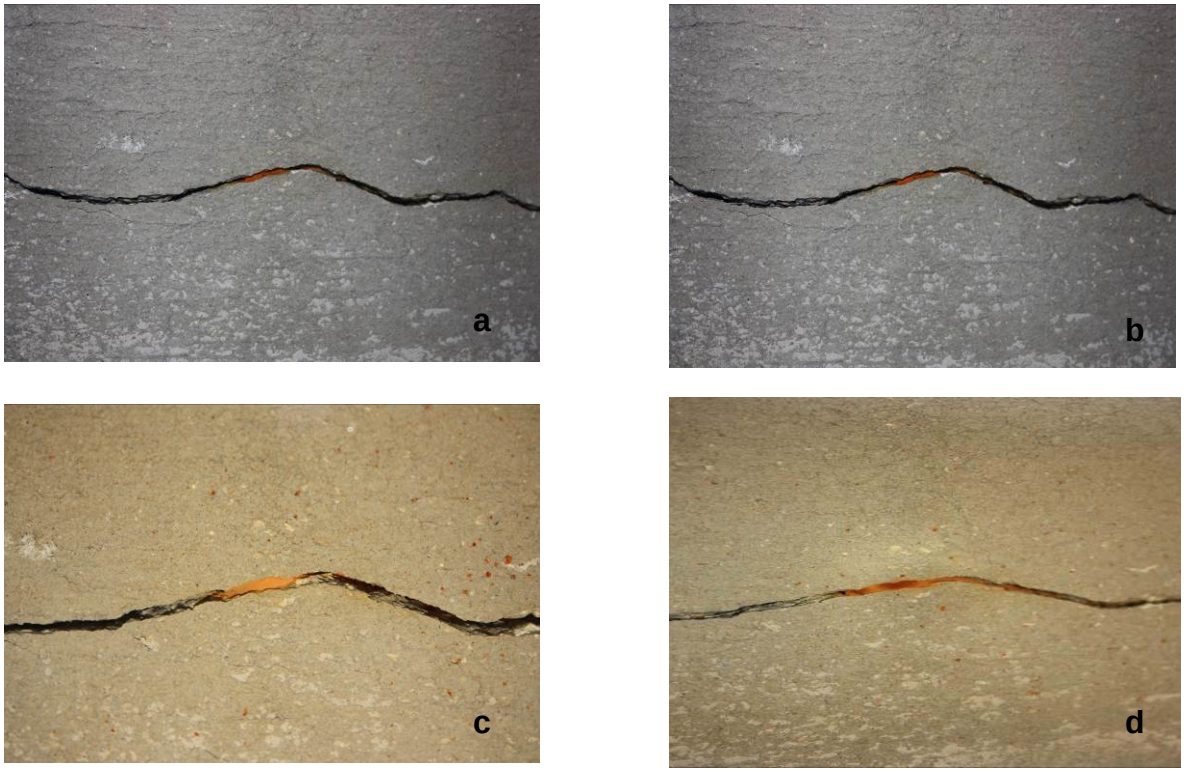

Figure (4.9) Corrosion product evolution in specimen R12 (0.100-in-wide crack class) during exposure up to (a) 14 days (b) 20 days (c) 34 days (d) 52 days after the ponding solution started to incorporate chloride ion

Figure (4.10) Specimen R12 (0.100-in-wide crack class) showing a corrosion spot at a crack-steel wire intersection close to the specimen edge about 52 days after the ponding solution started to incorporate chloride ion

Figure (4.11) Specimen R4 (0.100-in-wide crack class) showing a corrosion spot at a crack-steel wire intersection close to the specimen edge about 52 days after the ponding solution started to incorporate chloride ion

Figure (4.12) Specimen Z14 (0.100-in-wide crack class) showing no corrosion product spots about 52 days after the ponding solution started to incorporate chloride ion

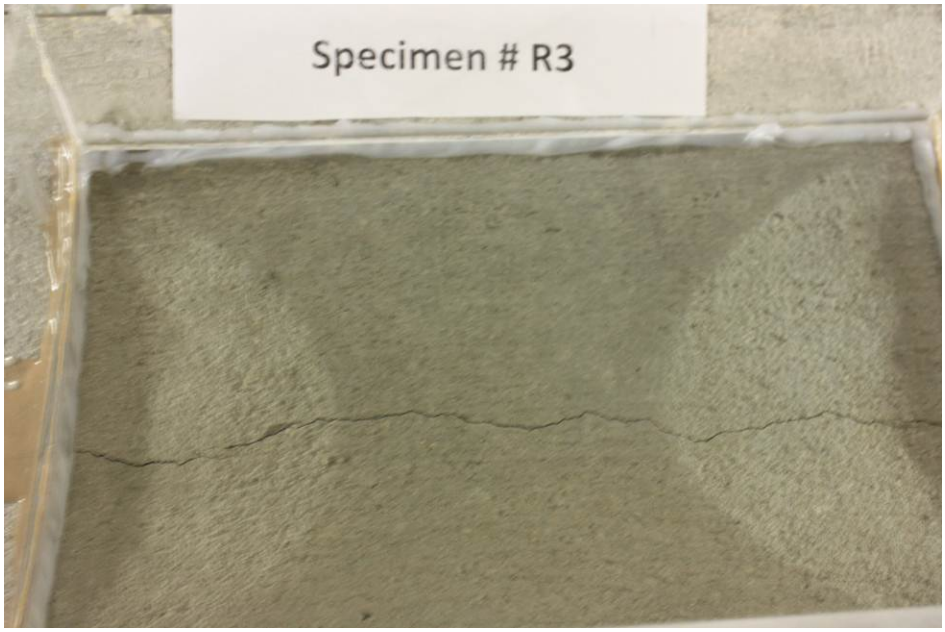

Figure (4.13) Specimen R3 (0.020-in-wide crack class) showing no corrosion product spots about 52 days after the ponding solution started to incorporate chloride ion

Figure (4.14) Specimen Z13 (0.020-in-wide crack class) showing no corrosion product spots about 52 days after the ponding solution started to incorporate chloride ion

4.2.2 Electrochemical Measurements

Open circuit potential (OCP) can serve as an indicator of corrosion condition (Sagüés 1993). As detailed in ASTM C-876 (ASTM 2009) highly negative potentials in atmospherically exposed concrete are symptomatic of ongoing active corrosion of concrete reinforcement, while less negative values are associated with passive, low corrosion rate conditions. Figure 4.15 shows the open circuit potential values averaged over each of the two exposure periods for all test conditions and for each pair of replicate test specimens. Replicate specimens yielded potential values comparable to each other. The control (uncracked) specimens from both manufacturers showed, as expected, less negative OCP values typical of those expected for passive steel in concrete. In contrast, the 0.100-in-width crack specimens showed highly negative potentials, even in the chloride-free initial exposure phase.

The OCP observations, along with the direct observations of rust noted above, support the concern stated in the Introduction chapter that steel exposed at the bottom of relatively large cracks faces a solution that is much less alkaline than the pore water of the concrete. That condition is likely the result of efficient diffusional and convective mixing inside the wide crack between any leachates from the concrete pore waters at the crack walls, and the exterior water. The resulting electrolyte pH is not sufficient to create a stable passive regime even when no chloride ions are added. In such case, steel activation is possibly aided by the minimal native chloride content present in the concrete (Wang 2005). The presence of 500 ppm chloride aggravated conditions accordingly as evidenced by distinctly

more negative potentials. The OCP values for the 0.020 in-crack width-specimens were distinctly more negative than those of the uncracked controls, strongly indicating some extent of active corrosion as well even with the narrow cracks. The conditions responsible for activation are expected to be similar to that for the wider cracks. Some mitigation existed as the OCP values were not as negative as those for the wider crack specimens, likely indicating that activation at the bottom of the narrower cracks happened at fewer crack-steel wire intersection points, or that the size or the corrosion zones was smaller. Importantly, the OCP indications of corrosion were present regardless of the differences between the concrete compositions used by the suppliers.

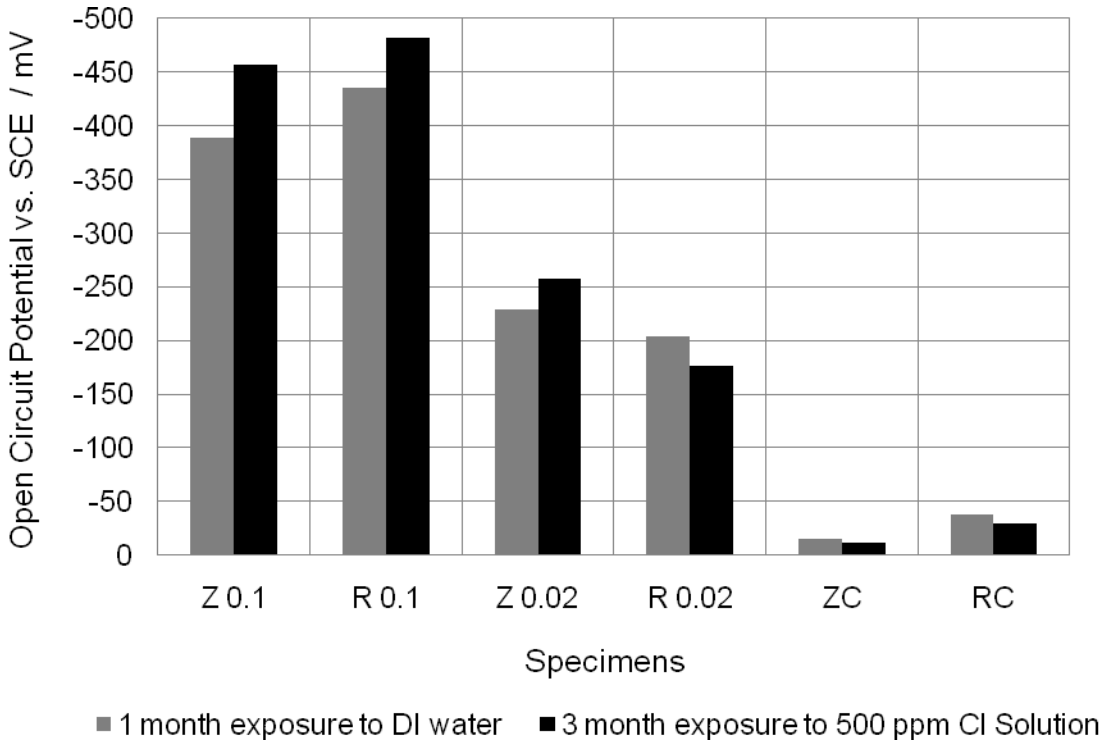

Figure (4.15) Average open circuit potentials over two exposure periods. Each data point is the average value of duplicate specimens over the indicated period

Further confirmation of the corrosion symptoms was provided by the EIS measurements, which gave as well quantitative estimates of the rate of steel corrosion to be used in the predictive modeling calculations detailed in the next chapter. Figure 4.16 exemplifies the EIS behavior of a cracked specimen during the distilled water (no added chloride) ponding period, 9 days after the exposure started. Figure 4.17 shows the EIS behavior of the same specimen 45 days during the period of ponding with 500 ppm chloride ion addition. The diagrams show EIS behavior that for the low frequency end of the spectrum could be approximated relatively well by the analog circuit in Figure 3.19 . The portion of the spectrum at frequencies higher than those of the last decade sampled could be fitted by the circuit analog only with varying degrees of success. As a first approximation, data for only the lowest decade of frequencies measured were used for evaluation of Rp in all the tests addressed in this report for which the circuit analog fit was used. The results have been archived for possible more detailed interpretation in the future. Given the approximate nature of the Rp evaluations using the circuit analog, and the further assumptions used for the cases using a proportionality factor PF, the Rp or Rpc values thus obtained and discussed in the following will be referred to as nominal polarization resistances. The corrosion currents evaluated using Eq.(3.3) will be treated accordingly as nominal values as well and their approximate nature recognized when interpreting the results.

With the above provisions, the nominal polarization resistance in Figures 4.16 and 4.17 is the distance between the high and low frequency intersections respectively with the horizontal (real) axis of the impedance diagram. The nominal polarization resistance for the data in Figure 4.17 (after chloride addition) is somewhat smaller than that for Figure 4.16 (before chloride addition), suggesting per application of Eq. (3.3) a correspondingly higher nominal corrosion rate in the former as expected. It is emphasized that given the uncertainties noted above, observations on corrosion behavior trends were based not only on the results of this particular pair of tests, but also on consideration of the results from multiple tests.

Figures 4.18 and 4.19 illustrate the EIS behavior of specimens that experienced very low to negligible nominal corrosion rates at the time of testing. The nominal value of Rp for specimen R6 (Figure 4.18) was extremely large so the impedance diagram is dominated by the straight-line characteristic response of the CPE (Sagüés 1993). The corresponding nominal corrosion current per Eq. (3.3) is nil. The nominal value of Rp for Z1 (Figure 4.19) was finite but still large and the fit line shows only very slight curvature. For the fast tests with lowest frequency <1mHz, where only crude estimates of Rp were made, similar circumstances were treated by reporting the Rp estimated value as “unlimited”.

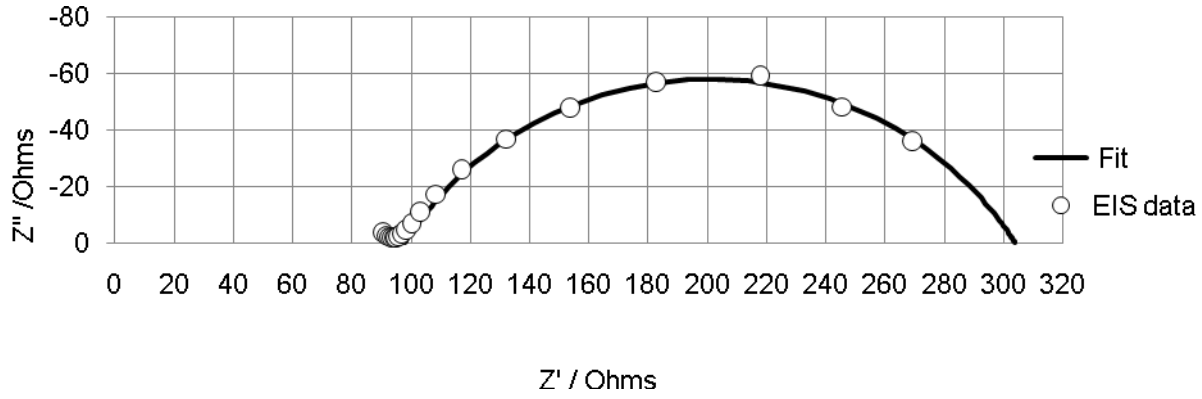

Figure (4.16) EIS behavior of specimen R12 (0.100 in crack) after 9-day ponding with DI water (no added chloride). Measured frequency range: 1 mHz to 1000 Hz, 4 points per decade. The solid line, extended to the zero frequency limit, is the fit obtained with the equivalent circuit when adjusting for the 1 mHz to 0.01 Hz data only.

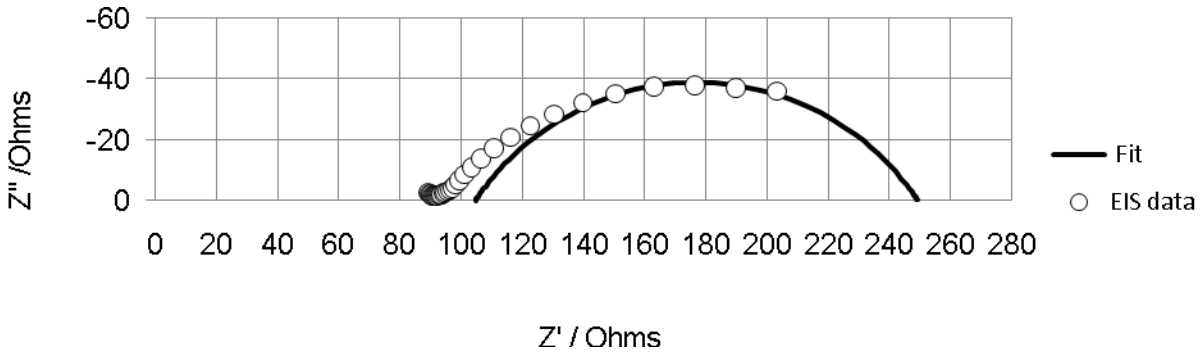

Fig. (4.17) EIS behavior of specimen R12 (0.100 in crack) after 45 days after the ponding solution started to incorporate chloride ion, over a frequency range of 1mHz to 1000 Hz, 5 points per decade, and the equivalent circuit fitting. The solid line, extended to the zero frequency limit, is the fit obtained with the equivalent circuit when adjusting for the 1 mHz to 0.01 Hz data only.

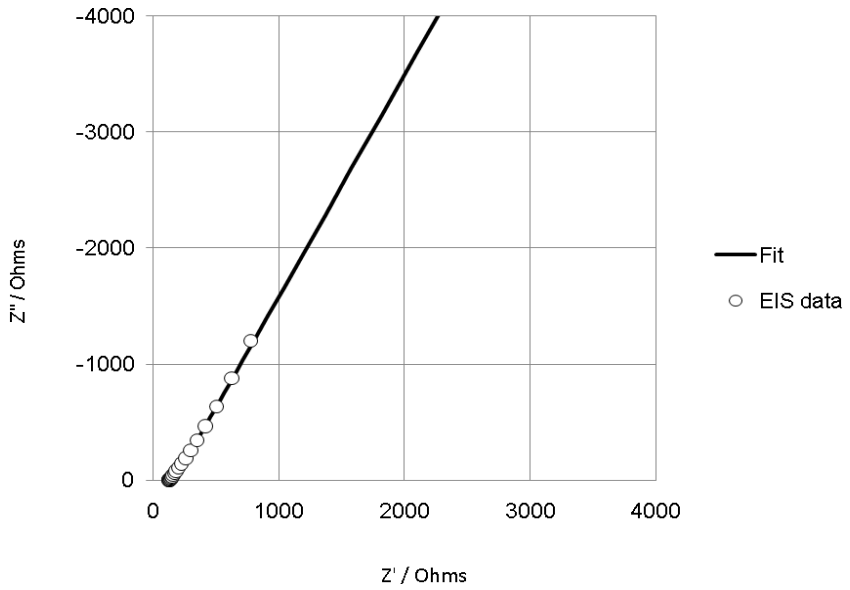

Fig. (4.18) EIS behavior of specimen R6 (0.020-in-crack class) after 45 days after the ponding solution started to incorporate chloride ion, over a frequency range of 1mHz to 1000 Hz, 5 points per decade. The solid line is the fit obtained with the equivalent circuit when adjusting for the 1 mHz to 0.01 Hz data only.

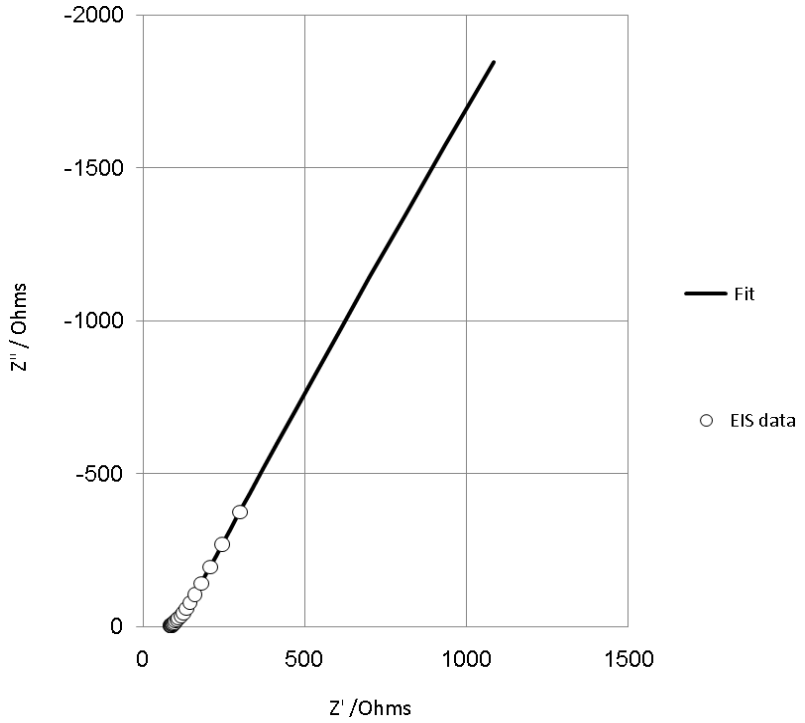

Fig. (4.19) EIS behavior of specimen Z1 (0.020-in-crack class) after 42 days after the ponding solution started to incorporate chloride ion, over a frequency range of1mHz to 1000 Hz, 5 points per decade. The solid line is the fit obtained with the equivalent circuit when adjusting for the 1 mHz to 0.01 Hz data only.

Table 4.1 summarizes the values of the fit parameters extracted from the EIS measurements of all the specimens tested during the periods before and after chloride ion addition. For the following discussion, only the value of nominal polarization resistance, which yields the nominal corrosion current, will be addressed. An average cluster test date was assigned to a group of measurements when it was conducted within a period of a few days. The corrosion current values for each cluster test date, averaged for the replicate specimens of each test condition, are displayed in Figure 4.20. The average values for the entire data set in each ponding condition are summarized in Figure 4.21. The results indicate trends in general agreement with those suggested by the OCP measurements and visual observations of rust: clear indications of ongoing corrosion for the wider crack specimens from both concrete mixtures, with greater severity occurring after the addition of chloride ions; some but significantly less corrosion present for the small crack width, and no measurable corrosion for the uncracked control specimens.

The nominal corrosion currents are integrated values that correspond to total metal loss per unit time, which can be obtained by means of the Faradaic conversion

$$dm/dt = I_{CORR}\, Aw_{Fe}\, F^{-1}\, v^{-1} \qquad \text{Eq.(4.1)}$$

Where dm/dt is the amount of steel loss due to corrosion in g/s; Aw_{Fe} is the atomic weight of Fe (assumed on first approximation to make up the entire steel mass), 55.847 g/mole; F is Faraday's constant, 96,485 coul/equivalent; and v is the effective valence corresponding to assuming that iron dissolves as divalent ions, 2.

Application of Eq.(4.1) to the data in Figure 4.21 indicates that during the chloride exposure period the 0.100-in-crack-width specimens were experiencing metal loss in the order of ~ 4 mg/day. After 1-2 months there would be in the order of 0.2 g of steel converted into rust. Given the expansive nature of steel corrosion products (Marcotte 2001) that mass loss corresponds to the production of, e.g., 0.100 cm^3 of rust. Such amount is consistent with the visual observation reported above of multiple rust spots during the period of exposure. Per Figure 4.21 it is also evident that nominal metal loss and consequent rust production would be about one order of magnitude lower for the 0.020 in-crack width-specimens than that for the 0.100-in-specimens, consistent with the absence of observation of rust in the former. It is noted that the experiments address only a limited testing period

The corrosion experiments showed that significant reinforcement wire corrosion could take place in a short time in pipe with 0.100-in-wide cracks, and that corrosion damage was considerable slower when the cracks were 0.020 in wide. Corrosion was aggravated by the presence of moderate chloride ion contamination, but active steel corrosion occurred even without it. The next chapter introduces a corrosion projection model to evaluate possible effects of the observed corrosion on pipe durability.

Table (4.1) Values of the fit parameters extracted from the EIS measurements

Control									
Z6					**ZB**				
t	R_S	R_P	Yo	n	t	R_S	R_P	Yo	n
8*	157	8E+10	0.021	0.522	22*	203	6 E+10	0.020	0.516
47**	190	5E+10	0.039	0.603	48**	145	2E+11	0.049	0.607
R7					**R10**				
t	R_S	R_P	Yo	n	t	R_S	R_P	Yo	n
9*	165	2E+12	0.015	0.645	22*	185	2E+4	0.010	0.565
46**	303	3E+11	0.020	0.695	48**	238	1E+11	0.013	0.579

0.020 in									
Z1					**Z13**				
t	R_S	R_P	Yo	n	t	R_S	R_P	Yo	n
8*	133	3.56E+3	0.060	0.554	5*	108	2.78E+3	0.050	0.505
42**	108	9.5E+4	0.084	0.703	42**	97	292	0.184	0.619
64**	130	2E+11	0.066	0.734	63**	114	318	0.149	0.598
R3					**R6**				
t	R_S	R_P	Yo	n	t	R_S	R_P	Yo	n
9*	108	4.85E+3	0.019	0.527	9*	123	2E+11	0.021	0.604
46**	141	3.14E+3	0.017	0.549	46**	171	2E+11	0.025	0.693
63**	163	2.88E+3	0.019	0.593	73**	181	6E+11	0.025	0.703
0.100 in									
Z11					**Z14**				
t	R_S	R_P	Yo	n	t	R_S	R_P	Yo	n
9*	70	127	0.081	0.457	4*	97	358	0.069	0.574
42**	65	65	0.289	0.495	42**	71	276	0.226	0.540
53**	63	204	0.108	0.275	54**	73	280	0.237	0.564
R12					**R4**				
t	R_S	R_P	Yo	n	t	R_S	R_P	Yo	n
8*	98	206	0.038	0.653	4*	94	450	0.022	0.593
46**	105	145	0.095	0.628	45**	94	226	0.037	0.499
55**	96	177	0.056	0.520	53**	107	207	0.101	0.577

Notes: * Exposure time in days to DI water before adding chloride; ** Exposure time in days to chloride solution after being exposed to DI water for 33 days; Rs: Solution resistance in ohms; Rp: Polarization resistance in ohms; Yo: CPE parameter in (sec^n/ohm); n: CPE parameter, dimensionless; Lowest frequency in EIS measurements, before and after Cl^- exposure, was 1 mHz or 0.2 mHz.

Table (4.2a) Estimated Rp for EIS data having lowest frequency > 1 mHz (uncracked)

Control									
Z6					**ZB**				
t	PF	Rs	Rpp	Rpc	t	PF	Rs	Rpp	Rpc
17*	4E+08	142	177	UNL	7**	7E+08	9E+01	246	UNL
6**	2E+08	127	290	UNL					
17**		133	296	UNL	17**		95	246	UNL
20**		140	302	UNL	20**		100	255	UNL
35**		142	293	UNL	35**		98	247	UNL
R7					**R10**				
t	PF	Rs	Rpp	Rpc	t	PF	Rs	Rpp	Rpc
17*	4E+09	158	417	UNL	6**	1E+08	145	700	UNL
6**	3E+08	172	818	UNL					
17**		196	1E+3	UNL	17**		163	745	UNL
20**		194	1E+3	UNL	20**		165	761	UNL
35**		210	827	UNL	35**		177	778	UNL

Table (4.2b) Estimated Rp for EIS data having lowest frequency > 1 mHz (0.020 in crack)

0.020 in									
Z1					**Z13**				
t	PF	Rs	Rpp	Rpc	t	PF	Rs	Rpp	Rpc
17*	42	122	87	3.5E+03	17*	16	103	175	3E+03
6**	456	77	131	6E+04	4**	4.3	76	80	347
14**		80	154	7E+04	13**		78	71	306
20**		82	170	7E+04	20**		78	69	297
34**		83	193	9E+04	34**		77	64	277
R3					**R6**				
t	PF	Rs	Rpp	Rpc	t	PF	Rs	Rpp	Rpc
17*	22	124	230	5.1E+03	17*	6E+08	120	278	UNL
6**	6.56	108	400	2.6E+03	6**	2E+08	100	527	UNL
13**		118	430	2.8E+03	14**		107	570	UNL
20**		116	400	2.6E+03	20**		108	593	UNL
34**		126	426	2.8E+03	34**		118	627	UNL

Table (4.2c) Estimated Rp for EIS data having lowest frequency > 1 mHz (0.100 in crack)

0.100 in									
Z11					**Z14**				
t	PF	Rs	Rpp	Rpc	t	PF	Rs	Rpp	Rpc
17*	3.58	80	39	140	17*	5.06	87	40	202
6**	2.32	48	25	57	6**	6.56	57.	48	317
13**		49	25	58	13**		59	52	343
20**		50	23	54	20**		59	51	333
34**		50	26	60	34**		61	43	283
R12					**R4**				
t	PF	Rs	Rpp	Rpc	t	PF	Rs	Rpp	Rpc
17*	1.95	101	104	202	17*	2.57	98	122	312
6**	1.63	85	98	158	6**	2.10	86	133	278
13**		85	94	152	13**		96	108	227
20**		86	93	151	20**		94	110	232
34**		93	90	148	34**		107	108	225

Notes: * Exposure time in days to DI water before adding chloride; ** Exposure time in days to chloride solution after being exposed to DI water for 33 days; Rs: Solution resistance in ohms; Rpp: Provisional polarization resistance in ohms; PF: Proportionality factor; Rpc: Estimated polarization resistance in ohms; UNL: Denotes Rpc values greater than 10E7 ohm, effectively immeasurably high impedance indicative of a very low corrosion rate; Lowest frequency in EIS measurements before Cl^- exposure was 10 mHZ and after Cl^- exposure was 3 mHz.

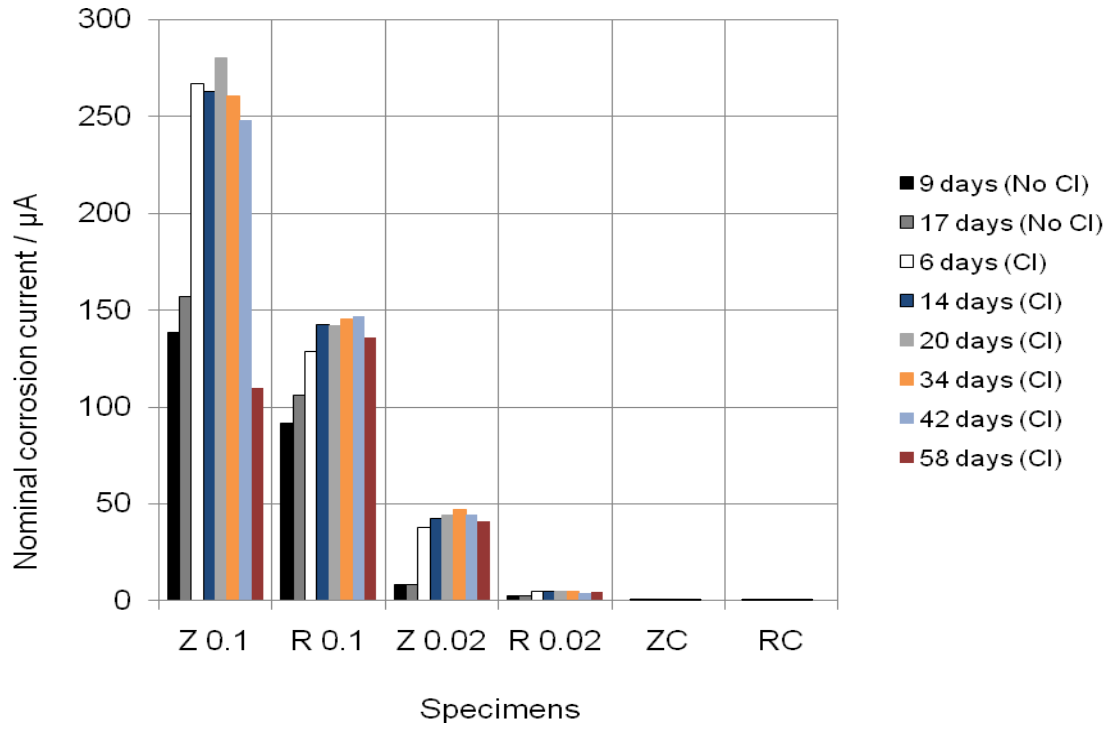

Figure (4.20) Nominal corrosion currents averaged for duplicate specimens, for 9 days and 17 days into the 33-day DI water pond period and for 6, 14, 20, 34, 42 and 58 days into the subsequent 500 ppm Chloride ion addition ponding period.

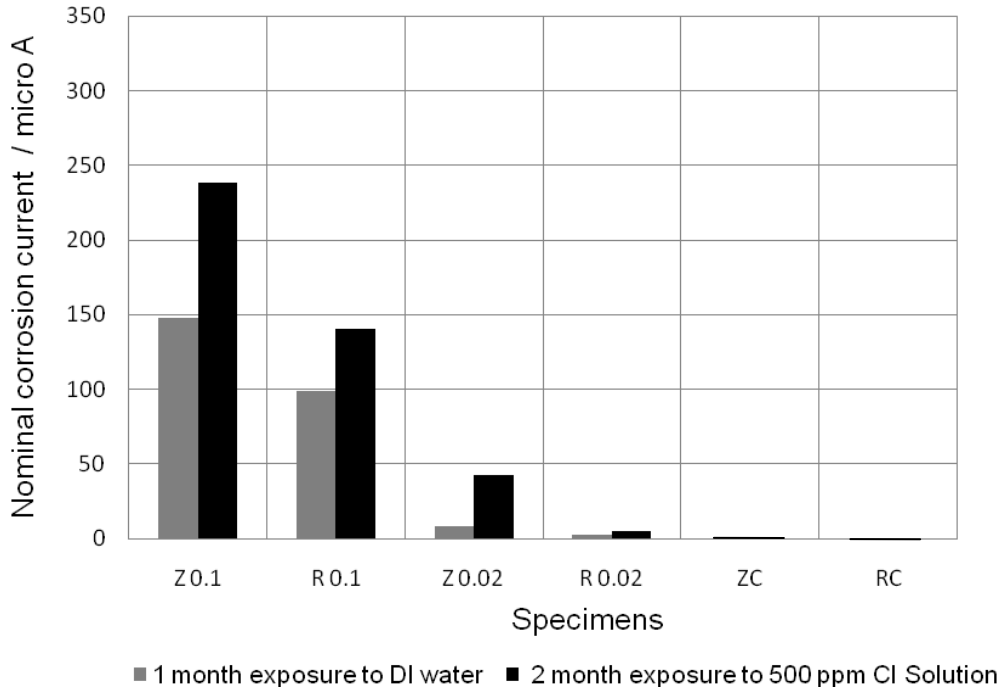

Figure (4.21) Average values of nominal corrosion currents over two exposure periods. Each data point is the average value of duplicate specimens over the indicated period

5 CORROSION DAMAGE FORECASTING MODELING

5.1 General Approach

The corrosion measurements described in the previous chapter provided an estimate of the amount of steel loss that was taking place as time progressed, for the various conditions evaluated. The physical effects of that corrosion, in particular the development of corrosion spalls or the loss of wire cross-section and consequent wire failure depend not only on the total rate of metal loss but also on how localized that loss may be. While the extent of corrosion localization is not precisely known, plausible assumptions of that extent can be made and used as the basis for corrosion damage forecasts based on possible scenarios. Those scenario-based projections give then an idea of the range of expected corrosion consequences to inform decisions leading to the development of a crack size acceptability criterion.

In the following, a modeling approach is presented and implemented to project the consequences of corrosion in cracked concrete pipe. The model starts from the approach used by the PI in previous work that evaluated the corrosion progression in cracked concrete (Lau 2010). The steel wire is assumed to have experienced local activation at the point where the crack intersects the wire. Activation is assumed to extent for a given distance on each side of the crack/wire intersections thus defining an active steel area for a given specimen size and wire placement density. The experimentally determined corrosion current is then divided by that total active area, resulting in a corrosion current density that is converted into a corrosion rate.

Calculations are then performed to assess durability under idealized failure scenarios. Actual performance reduction involves complex situations beyond those idealized scenarios. However, the quantitative estimates provided here serve to illustrate the time scales that may be involved for pipe performance failure and assessing impact of adopting alternative crack width criteria.

In one set of idealized calculations the repair-free service life of the pipe is assumed to have been reached when substantial reinforcing wire cross-section loss causes wire breaking due to mechanical overload, which would translate into reduction of mechanical strength of the pipe. For those calculations the corrosion rate is used to evaluate how long it takes until wire cross-section reaches a critical fraction of the initial value.

In alternative idealized calculations the event triggering need for repair is widespread concrete spalling, with consequent deterioration of hydraulic performance. For these calculations the corrosion rate value, together with the wire size, concrete cover and active zone size is the used to calculate using the relationship developed by Torres (2004) the time of service at which concrete spalls would develop.

5.2 Basic Modeling Statements

The following definitions, assumptions and simplifications apply:

1. Preexisting longitudinal cracks are present in reinforced concrete pipe specimens. A crack extends along the entire length, L, of a specimen. Figure 5.1 shows specimen and crack details.

2. The preexisting crack has a surface width, W.

3. All cracks intersect the embedded reinforcing steel wires.

4. The portion of longitudinal reinforcing steel wire within a specimen has a length, L and the portion of circumferential reinforcing steel wire has a length, C.

5. The number of longitudinal wires within a specimen footprint is n_L and the number of circumferential wires is n_c.

6. The total length of reinforcing wires within a specimen is $L_t = n_L L + n_c C$. The total surface area of steel wire within a specimen is $A_t = \pi D L_t$, where D is the reinforcing wire diameter.

7. The portion of reinforcing wire subject to corrosion when a preexisting crack intersects a wire crosswise has a length of influence, $2L_i$. The total surface area of wire subject to corrosion is, $A_i = n_x \pi D 2L_i$, Where n_x is the number of points where a crack intersects with a steel wire crosswise. The case of a crack that intersects or is in close proximity with a longitudinal wire is considered in the model input by changing the length of influence, $2L_i$.

8. The average concrete cover thickness is X_c with a standard deviation *Stdev*.

9. The average corrosion current calculated from EIS measurements is I_{corr}. This average corrosion current, $I_{corr,}$ is assumed to be made up of the sum of the current from passive regions, I_{pc}, and the current from the active regions, I_A. The active region area is assumed to be A_i as defined above and the passive region area is A_t-A_i.

10. The value of passive current per unit surface area of steel wire is $i_{p,}$ and is called the passive current density. The passive current density dominating passive regions in cracked specimens is assumed to have the same value as that of the passive current density in uncracked specimens.

11. In uncracked specimens, the average current calculated from impedance response measurements is I_{pu}, where the passive current density is given by $i_p = I_{pu}/A_t$ and therefore the passive current in cracked specimens may be determined by $I_{pc} = i_p(A_t - A_i)$.

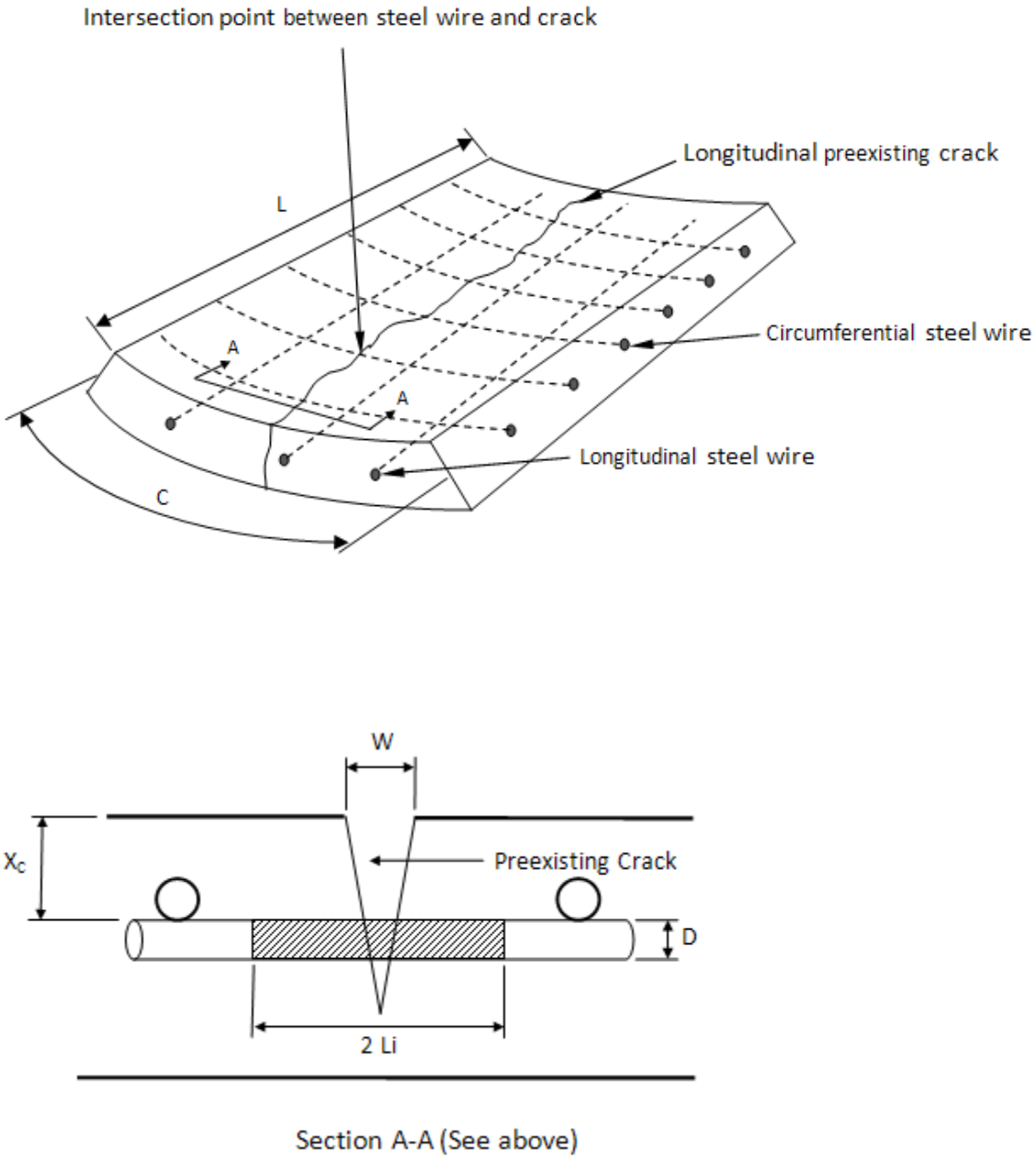

Figure (5.1) Schematic of a specimen of a reinforced concrete culvert pipe and illustration for crosswise intersection of reinforcing wire by preexisting crack

12. The active corrosion current in a cracked specimen is given by $I_A = I_{corr} - I_{pc}$.

13. The active corrosion current density is given by $i_A = I_A/A_i$ and assumed to be constant with time over the projected time span.

14. Corrosion creates expansive products that further crack/spall the concrete cover around the region of the preexisting crack. The corresponding amount of corrosion is expressed in terms of a critical amount of metal loss in the wire, $X_{crit.}$ On first approximation it is assumed that the model by Torres (2004) for previously uncracked concrete also applies here:

$$X_{crit}/mm = 0.11\ (X_c / D)\ (1+X_c/2Li)^2 \qquad \text{Eq. (5.1)}$$

15. The time to failure in years is projected for two alternative damage modes:

    a) Failure results from wire breaking due to mechanical overload when wire experiences a critical cross-section loss, expressed as a percentage CSL% of the initial cross-section. The corresponding time to failure is called t_{f1}.

    b) Failure results from concrete spall due to generation of further cracking arising from formation of expansive corrosion products. The corresponding time to failure is called t_{f2}.

    - It is assumed that crack-induced corrosion of steel wires in (b) would result in the generation of new cracks in surrounding concrete leading to accelerated concrete spalls rather than causing the preexisting crack to grow in width.

    - The active corrosion current density in the above two damage modes was assumed to be constant with time over the projected service life span.

    - If calculations reveal any values of projected time to failure exceeding 100 years, such values will be indicated as 100+ years.

5.3 Implementation

Based on the above assumptions and definitions, the time to failure in years, t_{f1} under wire failure alternative scenario is given by:

$$t_{f1} = (P\ v\ F\ \rho) / (i_A\ Aw_{Fe}) \qquad \text{Eq. (5.2)}$$

where Aw_{Fe}, v and F are defined in section 4.2.2; ρ is steel density, 7.8 g/cm^3; P is the penetration depth that results in steel wire failure, given by:

$$P = \frac{D}{2} - \sqrt{\frac{D^2(1-(CSL/100)\ )}{4}} \qquad \text{Eq.(5.3)}$$

Where CSL is a critical wire cross-section loss in %

For the concrete spall alternative scenario the time for failure in years t_{f2} is given by:

$$t_{f2} = (v\ F\ \rho\ X_{crit}) / (i_A\ Aw_{Fe}) \qquad \text{Eq.(5.4)}$$

5.4 Model Input Parameters and Cases Examined

Table 5.1 lists the input parameters and cases examined. Those cases correspond to the results for average nominal corrosion currents observed in the corrosion specimens evaluated in the laboratory, as summarized in Figure 4.21, but limited for brevity to the period following the beginning of chloride ion addition to the ponding water.

The calculations treated the corrosion length Li as a test parameter, with values ranging from small (Li = wire diameter) to large Li = 30 times the wire diameter, essentially corrosion nearly uniform as it may be the case with poor consolidation voids along much of the wire.

5.5 Model Results

5.5.1 Overall Qualification

It is important to emphasize that the model projections presented here result from idealized scenarios and assumptions that include extreme regimes and extrapolations not necessarily encountered in practice. Those extreme regimes serve as a bounding frame inside which the more plausible conditions may exist. The numeric service life projections given here are not engineering design outcomes, but rather serve for the comparative assessment of the effect of the variables of interest. It must be kept in mind also that the projections are based on the simplifying assumption that the corrosion rates encountered in a short laboratory test period would remain the same over service times that may involve many year decades. Thus, the projected times are only formal extrapolations and do not imply a particular advantage of one type of pipe manufacturer over the other. The labeling of the projections by Z- or R-type is made only to associate the projections with the variability of behavior that was encountered in the laboratory specimens, which is assumed to reflect to some extent the variability that may be encountered under normal production and use of pipe materials.

All service life projections discussed next must be qualified per the above provisions.

Table (5.1) Input parameters and cases considered

	Type of RC culvert pipe specimen	Z	R
D	Steel wire diameter	5 mm	
L	Longitudinal length of specimen	18 in	
C	Circumferential length of a specimen	16 in	
n_L	Number of longitudinal wires within a specimen	3	2
n_C	Number of circumferential wires within a specimen	6	5
n_X	Number of circumferential wires intersecting a crack	4	4
W	Average surface width of preexisting crack	0.020 in and 0.100 in	
2Li	Portion of steel wire influenced by corrosion Li = 1D Li = 2D Li = 5D Li = 10D Li = 20D Li = 30D	 2Li = 10 mm 2Li = 20 mm 2Li = 50 mm 2Li = 100 mm 2Li = 200 mm 2Li = 300 mm	
Xc	Average Concrete Cover Thickness / mm	30.75	17.97
Stdev	Concrete cover standard deviation / mm	7.98	4.32
CSL	Critical Cross-section loss	25 %, 50 % and 75 %	
	Exposure Environment	500 ppm Chloride , pH ~ 9	
	Exposure Period	~ 2 months	
ip	Average passive current density of uncracked specimens from EIS measurements ($\mu A/cm^2$)	0	0
I_{Corr}	The average corrosion current of cracked specimens from EIS measurements (μA) Specimens having a crack width 0.100 in Specimens having a crack width 0.020 in	 238 43	 140 5

5.5.2 Wire Failure Alternative Scenario.

Tables 5.2 and 5.3 show the projected service time duration for long and short corrosion influence lengths respectively. The calculations assumed that wire failure when half of the wire cross-section is lost, but trial evaluations showed comparable general trends when other criteria, e.g., 75% or 25% cross-section loss, were assumed.

If corrosion is not highly localized the projected wire failure event tends to be several year decades into the future except for the most severe corrosion case observed in the laboratory (Z-type with 0.100-in-wide cracks). Projected failure times for the 0.002-in-wide crack cases without highly localized corrosion approach or exceed 100 years in all cases.

The projections become significantly more pessimistic for the 0.100-in- wide cracks if corrosion is highly localized, with times to failure ranging from 2 to 14 years. For the 0.020-in cases the prognosis remains optimistic (near or above 100 years) for R-type but times to failure of only two decades on average are projected for Z-type.

It is noted that the Z-type material tested showed significant consolidation voids next to the wires, as shown in Figures 3.10 and 3.11. Thus the amount of metal exposed to solution may have been greater for this material and accounted for the greater corrosion currents observed for the Z-type specimens. At the same time, because the voids run along the wires the corrosion influence length for the Z-type specimens would be expected to be quite large, so for Z-type the more adequate projections would be those in Table 5.2.

From the above considerations, the overall projection from the wire failure scenario is corrosion-related durability in the order of up to some year decades for the 0.100-in-wide cracks, and little limitation (near or above 100 years) for the 0.020-in-wide crack cases.

Table (5.2) Model output: Wire failure scenario, long corrosion influence lengths

Time to Wire Cross-section Loss / Years				
Damage Mode	**50% CSL**			**Nominal Corrosion Current / µA**
Influence (2Li)/mm	*Li = 10D*	*Li = 20D*	*Li = 30D*	
	100	*200*	*300*	
Z (0.100 in)	28	56	84	238
Z (0.020 in)	92	100+	100+	43
R (0.100 in)	28	56	84	140
R (0.020 in)	100+	100+	100+	4.6

Table (5.3) Model output: Wire failure scenario, short corrosion influence lengths

Time to Wire Cross-section Loss / Years				
Damage mode	**50% CSL**			**Nominal Corrosion Current / µA**
Influence (2Li)/mm	*Li = 1D*	*Li = 2D*	*Li = 5D*	
	10	*20*	*50*	
Z (0.100 in)	3	6	14	238
Z (0.020 in)	9	18	46	43
R (0.100 in)	3	6	14	140
R (0.020 in)	85	100+	100+	4.6

5.5.3 Concrete Spall Alternative Scenario.

Table 5.4 summarizes the results for this assumed failure mode, estimated using the average concrete cover values for each pipe type. For this mode, each entry indicates the estimated amount of time required for the formation of cracks additional to the one already present at the beginning. Those additional cracks would create a concrete spall with consequent debris and increased surface roughness that degrade hydraulic performance. The additional cracking results from the stresses created by the expansive corrosion products when the local steel consumption reaches a critical penetration depth Xcrit.

Table (5.4) Model output: Concrete spall scenario, various corrosion influence lengths based on average concrete cover Xc

Time to Additional Concrete Cover Cracking / Years (based on average cover, Xc)							
Influence (2Li)/mm	*Li=1D*	*Li=2D*	*Li=5D*	*Li=10D*	*Li=20D*	*Li=30D*	**Nominal Corrosion Current / µA**
	10	*20*	*50*	*100*	*200*	*300*	
Z (0.100 in)	3	2	2	3	4	6	238
Z (0.020 in)	14	11	11	15	23	31	43
R (0.100 in)	1.2	1.1	1.4	2	4	5	140
R (0.020 in)	36	34	43	65	100+	100+	4.6

Table (5.5) Model output: Concrete spall scenario, various corrosion influence lengths based on Xc + Stdev

Time to Additional Concrete Cover Cracking / Years							
Influence (2Li)/mm	*Li=1D*	*Li=2D*	*Li=5D*	*Li=10D*	*Li=20D*	*Li=30D*	**Nominal Corrosion Current / µA**
	10	*20*	*50*	*100*	*200*	*300*	
Z (0.100 in)	5	3	3	4	6	7	238
Z (0.020 in)	26	19	17	21	31	41	43
R (0.100 in)	2	1.7	2	3	5	7	140
R (0.020 in)	60	52	60	86	100+	100+	4.6

Table (5.6) Model output: Concrete spall scenario, various corrosion influence lengths based on Xc - Stdev

Time to Additional Concrete Cover Cracking / Years							
Influence (2Li)/mm	*Li=1D*	*Li=2D*	*Li=5D*	*Li=10D*	*Li=20D*	*Li=30D*	**Nominal Corrosion Current / µA**
	10	*20*	*50*	*100*	*200*	*300*	
Z (0.100 in)	1	1	1	2	3	4	238
Z (0.020 in)	7	6	7	10	16	22	43
R (0.100 in)	0.6	0.7	0.9	1	3	4	140
R (0.020 in)	20	20	29	46	81	100+	4.6

As shown in Eq. (5.1) the value of Xcrit is larger the smaller the corrosion influence length. Ideally, if the corrosion influence length were small enough, complete corrosion of that part of the wire could take place without additional cracks being created in that extreme limit case. Conversely, for a given amount of corrosion

current, the value of the corrosion penetration X is greater the smaller the corrosion influence length. Consequently, for a given corrosion current the projected time to failure for this scenario has a minimum at a certain corrosion influence length and increases for greater and smaller influence lengths. The projections obtained here include the combined action of those effects and are reported without further elaboration given the scope of the present work.

Keeping the above considerations in mind, for the entire range of assumed influence length values the results in Table 5.4 project very short times (5 years or less) to additional cover cracking, if the preexisting crack width is 0.100 in. The prognosis becomes significantly better (several decades and greater) for the 0.020-in-crack width for the R-type pipe and for all influence zone sizes assumed. For the Z-type pipe the prognosis for the 0.020 in-crack width increases to 2 or more decades for the larger influence length values only, but it is recalled that this condition is the more likely for this pipe given the extended lengthwise consolidation voids noted earlier.

Due to the form of Eq. (5.1) the outcome of the concrete spall scenario depends on the value of the concrete cover too. To explore the influence of this parameter on the projections, additional calculations were made assuming that the concrete cover was one standard deviation thicker and thinner than the average for each type of pipe. Tables 5.5 and 5.6 show the results of the respective calculations. Each of those variations, representative of expected typical deviations from the average, resulted in changes in the projected times by about factor of 2 greater (for the thicker cover case) or smaller (thinner cover) than those calculated for the average cover. However, relative trends remained essentially the same with the projections for the 0.100-in-wide cases being much shorter than for the 0.020-in-wide cases and with the other relative differences between both types of pipe generally preserved as well. Given the uncertainty associated with the model assumptions and the observed variability in experimental corrosion behavior, such range in outcome while preserving relative trends does not substantially affect the overall conclusions that may be derived from consideration of the average case.

In summary, the concrete spall alternative scenario yields very short durability projections for the 0.100-in-wide crack condition, and moderately strong to little limitation in durability for the 0.020 in-wide crack cases.

5.5.4 Projections Based on the DI Water Exposure Period

The projections obtained above were made using the nominal corrosion currents obtained for the period when 500 ppm Cl^- ion addition to the DI water was taking place. However, as shown in Figures 4.20 and 4.21 and as suggested too by the OCP data, there was indication of appreciable corrosion during the plain DI water ponding period as well, roughly at about half the rate that was prevalent after chloride addition began.

Accordingly, for exposure to nearly chloride-free water the overall projections for both scenarios are more optimistic, by about a factor of two, than those for the chloride presence cases. However, considering the uncertainty inherent to this type of estimates such extension does not substantially alter the outcome that substantial loss of service life may result for the case of 0.100-in cracks, especially under the concrete spall scenario.

5.5.5 Spalling Versus Wire Break Alternative Scenario Impact.

The calculations projected generally earlier damage appearance by the concrete spall scenario than by the wire failure scenario. In addition to its earlier development, the spalling scenario merits the greatest consideration because of its associated negative effect on production of debris and increase in roughness both of which degrade hydraulic efficiency. In contrast, the argument has been made that the wire break scenario is little or only secondary importance, because the reinforcement is intended primarily to provide supplemental strength during transportation and placement, which is not necessary after the pipe is in place. Regardless of its merits, that issue becomes less relevant in view of the earlier projections of damage for the spalling scenario.

6 INTERPRETATION AND GUIDELINE MODELS

6.1 Interpretation of Findings

The findings from the literature review suggested that there was a reasonable expectation for autogenous healing to eventually occur for cracks narrower than about 0.020 in The prognosis was less favorable for wider cracks, and the evidence examined offered little assurance that autogenous healing would reliably take place for crack widths exceeding about 0.100 in. The crack healing laboratory experiments performed here do not appear to have been long enough to further elucidate that issue. A cautionary note however is in order, to the effect that even the narrowest (0.020 in wide) cracks evaluated failed to show clear signs of autogenous healing after about 2 months of testing.

The literature review revealed indications of lack of reinforcement corrosion even in 0.100-in-wide cracks, and even in the absence of autogenous healing, if the environment was low in chlorides. Those indications inspired guidelines such as those in AASHTO (2006) and Caltrans (2009), the latter of which allows 3 mm-wide (0.118 in) cracks for up to 500 ppm environmental Cl^-. Such approach was not supported by the present corrosion experiments, which showed indication of active and sustained corrosion for unhealed 0.100-in-wide cracks with 500 ppm Cl^- water. Estimates using a simplified forecasting model projected that under those conditions development of concrete spalls could occur after as little as a few years of service, a prognosis that did not improve dramatically even when no intentional chloride addition took place. The prognosis became substantially better when the results from the corrosion tests with 0.020-in–wide, unhealed cracks were considered. In those cases the projected times to spall were often not much lower than a typical target 100 year period, especially if the environment included no intentional chloride addition. Estimates made for an alternative adverse corrosion effect mode, wire failure, tended to yield longer effective service lives than for the concrete spall mode. However, as noted earlier the greatest adverse corrosion impact would be expected to be anyway from the earlier occurring spalling, with its associated hydraulic efficiency derating.

6.2 Guideline Models

As noted earlier, both the experimental work and the model projections were subject to considerable qualifications, serving mostly as supplementary material to that encountered in the literature review. With that provision, the overall findings suggest that in-place cracks up to 0.020 in wide at the inner surface of the pipe may be tolerable in moderately aggressive environments, given the expectation of eventual autogenous healing and the relatively low extent of corrosion in the laboratory tests even in the absence of prior healing. Wider cracks incur increasingly greater risk of significant corrosion service life derating, given the increasingly lower expectation of effective autogenous healing and the outcome of the corrosion tests. The laboratory corrosion testing results agree with indications from the literature

search, in suggesting that no consideration be given to acceptance of cracks wider than 0.100 in

Based on the above, development of a guideline for crack surface width acceptance for installed and backfilled RCP may proceed by discussion of the following alternative models. It is assumed that a highly accurate and reliable crack detecting and measuring RCP inspection methodology is available. In all cases the number and length of cracks allowable should have a specified upper limit, comparable to those used for acceptance of RCP before placement.

Model 1 - Most Restrictive:

Allowable width is 0.020 in when environmental chloride content is no greater than 500 ppm. Otherwise allowable width is 0.010 in (a value that is accepted before placement anyway).

Rationale: reasonable likelihood of autogenous healing and only minor corrosion effects observed in laboratory testing. No allowance for higher chloride content is made in absence of direct laboratory evidence.

Model 2 - Moderately Restrictive:

Allowable width is 0.020 in when environmental chloride content is no greater than 2000 ppm. Otherwise allowable width is 0.010 in (value is accepted before placement anyway).

Rationale: reasonable likelihood of autogenous healing presupposes tolerance to higher environmental chloride content than that experienced in the laboratory testing with no healing. Limit is set to 2000 ppm based on potential for evaporative surface chloride buildup if that value is exceeded per Sagüés (2001). It is recommended that consideration of adoption of this alternative be made pending outcome of further corrosion testing.

Model 3 - Derating Restriction:

The provisions of Model 2 apply, with the exception that crack widths W_A between 0.020 in and 0.100 in are allowed as well. That allowance is made for that range provided that the estimated service life of the pipe, as evaluated by the FDOT Optional Pipe Material Handbook (FDOT 2008), is multiplied by a sliding factor F_S. The factor is calculated by Eq. (6.1)

$$F_S = (0.100 \text{ in} - W_A)/0.08 \text{ in} \qquad \text{Eq.(6.1)}^*$$

For widths less than 0.020 in, Eq.(6.1) is not used and Model 3 defaults to Model 2.

Rationale: same as for Model 2 but allowing some credit for the possibility of autogenous healing acting as a mitigating factor for crack widths between 0.020 in and 0.100 in. The estimated service life reduces to zero for $W_A = 0.100$ in, effectively disallowing that value.

* This equation supersedes that in a previous version of the document.

7 CONCLUSIONS

1. A survey showed that few transportation agencies had maximum allowable crack width guidelines for in-place RC drainage pipes. AASHTO specifies a maximum in place width of 0.100 in for non-corrosive conditions and 0.010 in for corrosive conditions. The technical literature indicated a reasonable expectation for autogenous healing to eventually occur for cracks narrower than about 0.020 in The prognosis was less favorable for wider cracks, and the evidence examined offered little assurance that autogenous healing would reliably take place for crack widths exceeding about 0.100 in.

2. Laboratory experiments did not produce significant autogenous healing of 0.100 in or 0.020-in-wide cracks in reinforced concrete pipe specimens over an approximately 2-month-long period.

3. Corrosion tests showed that significant reinforcement wire corrosion could take place in a short time in reinforced concrete pipe with 0.100 in wide cracks, and that corrosion damage was considerably slower when the cracks were 0.020 in wide. Corrosion was aggravated by the presence of moderate chloride ion contamination (500 ppm), but active steel corrosion occurred even without it.

4. A predictive model for corrosion development in cracked reinforced concrete pipe was formulated and applied to interpret the outcome of the laboratory corrosion tests. For 500 ppm chloride, the overall projection for a wire loss-of-cross-section failure scenario was corrosion-related durability in the order of up to some year decades for the 0.100 in wide cracks, and little limitation (near or above 100 years durability) for the 0.020-in-wide crack cases. A concrete spall failure scenario, deemed to represent the most adverse corrosion consequences, yielded very short durability projections for the 0.100-in-wide crack condition, and moderately strong to little limitation in durability for the 0.020-in-wide-crack cases.

5. Acceptable crack width guideline models proposed for discussion included a restrictive alternative, with 0.020 in width allowable only for environmental chloride no greater than 500 ppm; a less restrictive alternative allowing 0.020 in up to 2000 ppm chloride; and a sliding option for up to 2000 ppm chloride where pipe service life is progressively derated to zero for cracks widths increasing from 0.020 in to 0.100 in. In all models the acceptable width defaulted to 0.010 in. if the other conditions were not met.

8 REFERENCES

AASHTO (American Association of State Highway and Transportation Officials) (2006), LRFD Bridge Construction Specification, Section 27, Concrete Culverts, Clause (27.4.1), Washington DC.

ACI Committee 224, (1998), “Causes, Evaluation and Repair of Cracks in Concrete Structures”, ACI 224.1R-93, Re-approved.

ACPA (American Concrete Pipe Association) (2007a), “Cracks in Installed Reinforced Concrete Pipe”, Resource # CP info 02-712 (09/07), http://www.concrete-pipe.org,.

ACPA (American Concrete Pipe Association) (2007 b), “Effects of cracks in reinforced concrete sanitary sewer pipe”, Resource # 02-712 (09/07), http://www.concrete-pipe.org.

ACPA (American Concrete Pipe Association) (2007 c), “Effects of cracks in reinforced concrete culvert pipe”, Resource # 02-712 (09/07), http://www.concrete-pipe.org.

Alahmad, S., Toumi, A., Verdier, J. and Francois, R.(2009) "Effect of crack opening on carbon dioxide penetration in cracked mortar samples", *Materials and Structures*, Vol. 42, p. 559.

Allan, M. and Cherry, B. (1991), “Factors Controlling the Amount of Corrosion for Cracking in Reinforced Concrete”, Paper No. 125, Corrosion/91, NACE International, Houston, Texas.

Allan, M. and Cherry, B. (1989), “Mechanical Simulation of Corrosion Induced Cracking in Reinforced Concrete”, Paper No. 377, Corrosion/91, NACE International, Houston, Texas.

Alonso C., Andrade C., Rodriguez J. and Diez J.M. (1998), “Factors controlling cracking of concrete affected by reinforcement corrosion”, *Materials and Structures*, Vol.31, p. 435.

Andrade, C and Gonzalez, J. A. (1978), “ Quantitative measurements of corrosion rate of reinforcing steels embedded in concrete using polarization resistance measurements”, *Werkstoffe und Korrosion* Vol. 29, p.515.

ASTM (2009), C876 – 09 “Standard Test Method for Half-Cell Potentials of Uncoated Reinforcing Steel in Concrete”, American Society for Testing and Materials, Philadelphia, PA.

ASTM (2011), C76 – 11 “Standard Specification for Reinforced Concrete Culvert, Storm Drain, and Sewer Pipe”, American Society for Testing and Materials, Philadelphia, PA.

AWWA (American Water Works Authority) (1999), Standard C301-99 – Pre-stressed Concrete Pressure Pipes, Steel-Cylinder Type, for Water and Other Liquids. (Section 4.6.10.2), Denver-Colorado.

AWWA (American Water Works Authority) (2007), Standard-C205 “Cement mortar protective lining and coating for steel water pipe-4 in and larger- shop applied”, (Section 4.4.6.2), Denver-Colorado.

Bentur, A. and Mitchell, D. (2008), "Material performance lessons”, *Cement and Concrete Research* Vol. 38, p. 259.

Bhargava, K., Ghoshb, A., Mori, Y. and Ramanujama, S. (2006), “Analytical model for time to cover cracking in RC structures due to rebar corrosion”, *Nuclear Engineering and Design*, Vol. 236, p. 1123.

Bhargava, K., Ghoshb, A., Mori, Y. and Ramanujama, S.(2005), “Modeling of time to Corrosion-Induced Cover Cracking in Reinforced Concrete Structures”, *Cement and Concrete Research*, Vol. 35, p. 2203.

Bhargava, K., Ghoshb, A., Mori, Y.and Ramanujama, S. (2006), “Model for cover cracking due to rebar corrosion in RC structures”, *Engineering Structures*, Vol. 28, p.1093.

Buyle-Bodin, F., Thang, A., Dekoster, M., Blanpain, O., Maurel, O. (2005), Modeling of Corrosion induced Failure of Reinforced Concrete Structures”, 10DBMC International Conference on Durability of Building Materials and Components, Lyon, France.

Cabrera, J. (1996), “Deterioration of Concrete Due to Reinforcement Steel Corrosion”, *Cement & Concrete Composites*, Vol.18, p. 47.

Caltrans (2009), Caltrans Construction Manual, Chapter 4, section 65-reinforced concrete pipe, http://www.dot.ca.gov/hq/construc/manual2001/cmaug2009withbookmarks.pdf,

Capozucca, R. (1995), “Damage to Reinforced Concrete Due to Reinforcement Corrosion”, Construction *and Building Materials*, Vol. 9, No. 5, p. 295.

Carette, G., Bilodeau, A. (1993), Chevrier, R., and Malhotra, V., “Mechanical Properties of Concrete Incorporating High Volumes of Fly Ash from Sources in the U.S.”, *ACI Materials Journal*, Vol. 90-6, p 535.

Castorena, J., Almeraya-Caderon, F., Velasquez, J, gaona-Tiburcio, C., Cardenas, A., Barrios, C., Lopez, L. and Martinez, A. (2008), “Modeling the Time - to - Corrosion Cracking of Reinforced Concrete Structures by Finite Element”, *Corrosion Journal*, Vol. 64-7, p.600.

Chang, C. and Lien, H. (2007), “Expansion Stress Analysis of Ferroconcrete Corrosion by Digital Reflection Photoelasticity”, *NDT&E International*, Vol. 40, p. 309.

Chen, D. and Mahadevan, S. (2008), “Chloride-induced reinforcement corrosion and concrete cracking simulation”, *Cement & Concrete Composites*, Vol. 30, p. 227.

Chun-Qing, Li., Yang, Y., and Melchers, R. (2008), “Prediction of Reinforcement Corrosion in Concrete and Its Effects on Concrete Cracking and Strength Reduction”, *ACI Materials Journal*, Vol. 105, p.3.

CPAA (Concrete Pipe Association of Australasia) (2004), "Autogenous Healing", Technical Brief, NSW, Australia.
http://www.concpipe.asn.au/Tech_Info/PDFs/Briefs/TB12_07.pdf .

CPAA (Concrete Pipe Association of Australasia) (2008a), “Engineering Assessment and Acceptance Guideline - Circumferential Cracking”, St Leonards, NSW, Australia.

CPAA (Concrete Pipe Association of Australasia) (2008b), “Engineering Assessment and Acceptance Guideline - Longitudinal Cracking”, St Leonards, NSW, Australia.

Dhir, R., Sangha, C. and Munday, J.(1973), “Strength and Deformation Properties of Autogenously Healed Mortars”, *ACI Journal, Proc.* , Vol.70-24, p. 231.

Edvarsen, C.(1999), "Water Permeability and Autogenous Healing of Cracks in Concrete", *ACI Materials Journal*, Vol. 96, p. 448.

El Maaddawy, T., Soudki K., (2007) “A model for prediction of time from corrosion initiation to corrosion cracking”, *Cement & Concrete Composites*, Vol. 29, p. 168.

Elias, V. (2000), "Corrosion/Degradation of Soil Reinforcements for Mechanically Stabilized Earth Walls and Reinforced Soil Slopes", Publication No. FHWA-NHI-00-044, Federal Highway Administration, Washington, D.C.

FDOT (Florida Department of Transportation) (2010) “Standard Specifications for Road and Bridge Construction” Tallahassee, FL.
http://www.dot.state.fl.us/specificationsoffice/Implemented/SpecBooks/

FDOT (2009), Installed Pipe Cracking Survey Results, correspondence from M. A. Paredes to A. A. Sagüés, Nov. 9, 2009.

GMRA (Great Man-Made River Authority) (2007), Phase III - AlGardabiya and Assdada pump stations project- Report 1 “Overview of CML performance and summary of site visit, May 2007”, unpublished document, Benghazi.

Gonzalez, J., Andrade, C., Alonso, C., and Feliu, S. (1995), “Comparison of Rates of general Corrosion and maximum Pitting Penetration on Concrete Embedded steel Reinforcement”, *Cement and Concrete Research*, Vol. 25, p. 257.

Grimes, W., Hartt, W. and Turner, D. (1979), “Cracking of Concrete in Sea Water Due to Embedded Metal Corrosion”, *Corrosion*, Vol. 35, p.309.

Idrissi, H. and Limam, A. (2003), “Study and Characterization by Acoustic Emission and Electrochemical Measurements of Concrete Deterioration Caused by Reinforcement Steel Corrosion”, *NDT&E International*, Vol. 36, p. 563.

Ismail, M., Toumi, A., François, R. and Gagné, R. (2008), " Effect of Crack Opening on the Local Diffusion of Chloride in Cracked Mortar Samples" *Cement and Concrete Research* Vol. 38, 1106.

Jacobsen, S., Marchand, J and Boisvert, L. (1996), “Effect of Cracking and Healing on Chloride Transport in OPC Concrete”, *Cement and Concrete Research*, Vol. 26, p.869.

Jaffer, S. and Hansson, C. (2008), “The Influence of Cracks on Chloride-Induced Corrosion of Steel in Ordinary Portland Cement and High Performance Concretes Subjected to Different Loading Conditions”, *Corrosion Science*, Vol. 50, p. 3343.

Kim, C. Y. and Kim, J.K. (2008), “Numerical Analysis of Localized Steel Corrosion in Concrete”, C*onstruction and Building Materials*, Vol. 22, p.1129.

Kranc, S. C. and Sagüés, A. A. (1998), “Computation of Corrosion Distribution Of Reinforcing Steel in Cracked Concrete”, in Proc. International Conference on Corrosion and Rehabilitation of Reinforced Concrete Structures, Orlando, FL, Dec. 7-11, 1998, CD ROM Publication No. FHWA-SA-99-014, Federal Highway Administration.

Kuter, A. and Raupach, M. (2005), “Chloride Ingress in Concrete Cracks under Cyclic Loading”, Proceedings of ConMat’05, Third International Conference on Construction Materials: Performance, Innovations and Structural Implications, Vancouver, Canada.

Lau, K., Sagüés. A. and Powers, R. (2010), “Effect of Concrete Environment on the Corrosion Performance of Epoxy-Coated Reinforcing Steel”, *Corrosion*, Vol. 66, p. 065002.

Lazari, P., Gerard, B. (2000), “Mechanical Behavior of Corrosion Products formed at the Steel Concrete Interface- Testing and Modeling”. Conditions Monitoring of Materials and Structures. In: Proceedings EM2000, 14th Engineering Mechanics Conference, ASCE, Austin, TX, USA.

Li, Shu-cai, Wang, M. and Li, Shu-chen. (2008), “Model for Cover Cracking due to Corrosion Expansion and Uniform Stresses at Infinity”, *Applied Mathematical Modeling*, Vol. 32, p.1436.

Marcotte, T.D. (2001), “Characterization of Chloride-Induced Corrosion Products that Form in Steel-Reinforced Cementitious Materials, PhD Thesis in Mechanical Engineering., University of Waterloo: Waterloo, Canada.

McGuire, P., Harrison, N. (2004), “Concrete Storm Water Drainage Pipelines-Acceptance Using CCTV Inspection”, Concrete Pipe Association of Australasia, St Leonards, NSW.

Mohammed, T., Hamada, H. and Yokota, H. (2004a), “Autogenous Healing; Ingress of Chloride and Sulfate through Cracks in Concrete under Marine Environment”, *ACI Special publication*, Seventh CANMET/ACI International, May 2004, Las Vegas, U.S.A., Vol. 222-10, p. 135.

Mohammed, T., Hamada, H. and Yokota, H. (2004b), “Macro and Microcell Corrosion of Steel Bars in Cracked Concrete made with Various Cements”, *ACI Special publication*, Seventh CANMET/ACI International, May 2004, Las Vegas, U.S.A., Vol. 221-3, p. 51.

Montes, P., Bremner, T. and Lister, D. (2004), “Influence of Calcium Nitrite Inhibitor and Crack Width on Corrosion of Steel in High Performance Concrete Subjected to a Simulated Marine Environment”, *Cement & Concrete Composites*, Vol. 26, p.243.

Munoz, A., Andrade, C., Torres, A. (2007), “Corrosion Products Pressure Needed to Crack the Concrete Cover”, *Advances in Construction Materials*, ISBN-13 978-3-540-72447-6 Springer Berlin Heidelberg, New York, p. 359.

Neville, A. (2002), "Autogenous Healing - a Concrete Miracle?", *Concrete International*, Vol. 24, Issue 11, p. 76.

Ngab, A., Nilson, A. and Slate, F. (1981), “Shrinkage and Creep of High Strength Concrete”, *ACI Journal*, Vol. 78, No. 4, p. 255

OCPA (Ontario Concrete Pipe Association) (2000), Concrete Pipe design Manual, http://www.ocpa.com, Ontario.

Ohio DOT (Ohio Department Of Transportation) (2008),Supplemental Specification 802, “Post Construction Inspection of Storm Sewers and Drainage Structures”, April 15, 2005, supplemental to Construction and Material Specifications, (section 802.10, table 802.10.A), http://ftp.dot.state.oh.us/construction/OCA/Specs/SSandPN2008/802_04152005_for_2008.PDF.

Parks, J., Edwards, M., Vikesland, P., Fiss, M. and Dudi, A.(2008), “Autogenous Healing of Concrete in the Drinking Water Industry”, AWWA, Denver.

Pech-Canul, M. A. and Sagüés, A. A. (1999), “Evaluation of Steel Reinforcement Corrosion in Concrete Drainage M.A. Culverts”, Paper No. 563, Corrosion/99, NACE International, Houston, TX.

Poursaee, A., Hansson, C. (2008), “The influence of longitudinal cracks on the corrosion protection afforded reinforcing steel in high performance concrete”, *Cement and Concrete Research*, Vol. 38, p. 1098.

Ramm, W. and Biscoping, M. (1998), “Autogenous Healing and Reinforcement Corrosion of Water-Penetrated Separation Cracks in Reinforced Concrete", *Nuclear Engineering and Design*, Vol. 179 p. 191.

Raupach, M. (1996), “Chloride-Induced Macrocell Corrosion of Steel in Concrete – Theoretical background and practical consequences”, *Construction and Building Materials*, Vol. 10, No. 5, p. 329.

Raupach, M. (2006), “Models for The Propagation Phase of Reinforcement Corrosion – an Overview”, *Materials and Corrosion*, Vol. 57, No. 8, p.605.

Reinhardt, H. and Jooss, M. (2003), "Permeability and Self-Healing of Cracked Concrete as a Function of Temperature and Crack Width", *Cement and Concrete Research*, Vol. 33, p. 981.

Sagüés, A. A. (1989), “Corrosion Measurement of Aluminum Alloys and Reinforced Concrete for Determination of Culvert Service Life”, Final Report to Florida Dept. of Transportation Materials Office, Report No. 99700-7324-010.

Sagüés, A. A. (1993), “Corrosion Measurement Techniques for Steel in Concrete”, Paper No. 353, Corrosion/93, NACE International, Houston, TX.

Sagüés, A. A. (2003), “Modeling the Effects of Corrosion on the Lifetime of Extended Reinforced Concrete Structures”, *Corrosion*, Vol. 59, p.854.

Sagüés, A. A., Kranc, S. C. and Weyers, R. E. (2006), “In-Situ Leaching Method for Determination of Chloride in Concrete Pore Water” L. Cáseres, *Cement and Concrete Research*, Vol. 36, p. 492.

Sagüés, A. A., Peña, J., Cotrim, C., Pech-Canul, M. and Urdaneta, I. (2001), “Corrosion Resistance and Service Life of Drainage Culverts”, Final Report to Florida Dept. of Transportation, Report No.WPI 0510756, Contract No. B-9898.

Sagüés, A. (2008 a), Memorandum to B. Blanchard, FDOT, Feb. 24, 2008.

Sagüés, A. (2008 b), Letter to M. Paredes, FDOT, Dec. 9, 2008.

Sahmaran, M. and Özgür, I. (2008), “Influence of Transverse Crack Width on Reinforcement Corrosion Initiation and Propagation in Mortar Beams”, *Canadian Journal of Civil Engineering*, Vol. 35 No.3, p. 236.

Sahmaran, M. (2007), “Effect of Flexure Induced Transverse Crack and Self-Healing on Chloride diffusivity of reinforced mortar”, *J Mater Sci*, Vol.42, p. 913.

Saraswathy, V. and Song Ha-Won. (2007), “Evaluation of Corrosion Resistance of Portland Pozzolana Cement and Fly Ash Blended Cements in Pre-Cracked Reinforced Concrete Slabs under Accelerated Testing Conditions”, *Materials Chemistry and Physics*, Vol. 104, p356.

Song, H., Kim, H., Saraswathy, V. and Kim, T, (2007), “A Micro-mechanics Based Corrosion Model for Predicting the Service Life of Reinforced Concrete Structures”, *International Journal of Electrochemical Science*, Vol.2, p. 341.

Soylev, T. and Francois, R. (2003), “Quality of Steel–Concrete Interface and Corrosion of Reinforcing Steel”, *Cement and Concrete Research*, Vol. 33, p. 1407.

Tarek Uddin, M., Nobuaki, O., Hidenori, H. (2003 a), “Corrosion of Steel Bars in Cracked Concrete Under Marine Environment”, *Journal of Materials in Civil Engineering*, Vol. 15, issue 5, p 460.

Tarek Uddin, M. and Hamada, H. (2003 b), “Corrosion of Steel Bars in Concrete at Joints Under Tidal Environment”, *ACI materials Journal*, 100- M31.

Tarek Uddin, M., Nobuaki, O., Makoto H. and Tsunenori S. (2001), “Effect of Crack Width and Bar Types on Corrosion of Steel in Concrete”, *Journal of Materials in Civil Engineering*, Vol. 13, issue 3, p 194.

Torres-Acosta, A. and Sagüés, A. A. (2004), “Concrete Cracking by Localized Steel Corrosion - Geometric Effects”, *ACI Materials Journal*, Vol. 101, p.501.

Torres-Acosta, A., Gutierrez, S. and Guillen, J. (2007), “Residual flexure capacity of corroded reinforced concrete beams”, *Engineering Structures*, Vol. 29, p. 1145.

Torres-Acosta, A., Martinez-Madrid, M. (2003), “Residual Life of Corroding Reinforced Concrete Structures in Marine Environment”, *Journal of Materials in Civil Engineering*, Vol. 15, p. 344.

Torres-Acosta, A., Sagüés, A. A. (1998), “Concrete Cover Cracking and Corrosion Expansion of Embedded Reinforcing steel”, Rehabilitation of Corrosion Damaged Infrastructure, Chapter IV: Modeling, methods, techniques and technologies, p.215, NACE International, ISBN-970-92095-0-7.

Vidal, T., Castel, A., Francois, R. (2004), “Analyzing crack width to predict corrosion in reinforced concrete”, *Cement and Concrete Research*, Vol. 34, p.165.

Wang, H and Sagüés, A.A. (2005), “Corrosion of Post-Tensioning Strands”, Final Report to Florida Dept. of Transportation, Report No. BC353-33,, Nov 1.

Wilkins, N. and Stiliwell, J. (1986), “The Corrosion of Steel Reinforcement in Cracked Concrete Immersed in Sea Water, Marine Concrete, International Conference on Concrete in the Marine Environment, the Concrete Society.

Win, p., Watanabe, M., Machida, A. (2004), “Penetration Profile of Chloride Ion in Cracked Reinforced Concrete”, *Cement and Concrete Research*, Vol. 34, p. 1073.

Yang, Y. Z.; Lepech, M.; Yang, E. H.; and Li, V. C. (2009), “Autogenous Healing of Engineered Cementitious Composites under Wet-Dry Cycles”, *Cement and Concrete Research*, Vol. 39, p. 382.

Yuzer, N., Akoz, F., Kabay, N. (2008), “Prediction of Time to Crack Initiation in Reinforced Concrete Exposed to Chloride”, *Construction and Building Materials*, Vol. 22, p. 1100.